



# Soil erosion assessment using earth observation data in a trans-boundary river basin

Nirmal Kumar<sup>1</sup> · Sudhir Kumar Singh<sup>1</sup>

Received: 11 May 2020 / Accepted: 19 January 2021 / Published online: 21 February 2021  
© The Author(s), under exclusive licence to Springer Nature B.V. part of Springer Nature 2021

## Abstract

Soil erosion is a challenging environmental hazard that can be reduced by conservation practices. The study aimed to estimate the soil erosion rate using different digital elevation models (DEMs) data. We have applied the revised universal soil loss equation (RUSLE) to assess soil erosion in the Ghaghara river basin. We have also estimated morphometric parameters to understand the susceptibility of sub-basin to soil loss. The estimated rates of soil erosion by RUSLE are 21.39, 18.31, 4.35, and 4.64 ton/ha/year for SRTM 30 m, ALOS 30 m, MERIT 90 m, and SRTM 90 m, respectively. In addition to this water retention curve of soil was estimated using Hydrus-1D model. Result show that a clay\_loam soil has highest water holding capacity as 0.284 cm<sup>3</sup>/cm<sup>3</sup> and glacier (GLACIER-6998) has lowest as 0.22 cm<sup>3</sup>/cm<sup>3</sup>, respectively in the basin. Further the basin hypsometry analysis was performed using Q-GIS, which indicate that sub-basins age from young to mature due to soil erosion. In last, the prioritized map was generated by the integration of RUSLE, water holding capacity, and morphometry showed that the upper and middle portions of the basin need better conservation measures to control the excess soil erosion compared to the lower portion of the basin.

**Keywords** Hydrus · Hypsometry · Morphometry · Rainfall erosivity · RUSLE · Slope length · Soil erosion

## 1 Introduction

Rivers originated in Himalayan and Tibetan Plateau could supply almost 25% sediment load (Raymo and Ruddiman 1992). The lower parts of Himalayan sub-basin are now facing soil loss problems (Jain et al. 2001). The Shivalik formation (lower Himalaya), which is the source of Ganges river system, has weak geological combinations and, thus, susceptible to degradation environment and soil health. Therefore, it is vital to understand soil erosion, which will help to control erosion and ecological restoration. Soil is a natural resource, and natural and anthropogenic processes detach top surface

---

✉ Sudhir Kumar Singh  
sudhirinjnu@gmail.com

<sup>1</sup> K. Banerjee Centre for Atmospheric and Ocean Studies, University of Allahabad, Prayagraj 211002, Uttar Pradesh, India

of soil and aggravate soil erosion (Parveen et al. 2012). The natural resources and agricultural production are severely affected by the rapid action of soil erosion. The topography, low rainfall or prolonged dry periods, inept land use/land cover (Kumar et al. 2018a; Kumar et al. 2018; Bertalan et al. 2018), and natural calamities are different factors that determine the rate and process of erosion in a basin (Gitas et al. 2009). Kosmas et al. (1997) elaborated that basic properties of soil layer (upper soil thickness, silt, and organic matter percentage) are also responsible for severe erosion. Li and Fang (2016) explained that climate change directly alters trend and pattern of rainfall, and consequently due to intense rainfall, rate of runoff increases and accelerates soil erosion.

Remote Sensing and Geographic Information System (GIS) have been implemented in various available erosion models that predict soil loss (Borrelli et al. 2017; Uddin et al. 2016; Panagos et al. 2015a; Brady and Weil 2008). Currently, applications of remote sensing and GIS are a most appealing tool for natural resource management, complex hydrological problems and others (Rawat et al. 2020, 2019; Phinzi et al. 2020; Schlosser et al. 2020; Rawat et al. 2020; Barman et al. 2021; Singh and Singh 2018; Maliqi and Singh 2019; Bertalan et al. 2019; Choudhari et al. 2018; Abriha et al. 2018; Murmu et al. 2019; Kumar et al. 2017, 2018b; Thakur et al. 2016; Yadav et al. 2014). The uncertainty in digital elevation models (DEMs) may influence the results of hydrological investigations (Mondal et al. 2017). Many researchers have evaluated the accuracy of different DEMs (Szabó et al. 2015; Degetto et al. 2015; Rawat et al. 2019).

The Universal Soil Loss Equation (USLE; Wischmeier and Smith 1978), Chemicals, Runoff and Erosion from Agricultural Management Systems (CREAMS) (Knisel et al. 1980), Agricultural Non-Point Source Pollution (AGNPS) (Young et al. 1989), Revised Universal Soil Loss Equation (RUSLE) (Renard et al. 1991), and Modified Universal Soil Loss Equation (MUSLE) (Williams et al. 1975) are empirical models employed for soil erosion estimation. However, Morgan-Morgan and Finney (MMF) (Morgan et al. 1984), European Soil Erosion Model (EUROSEM) (Morgan et al. 1992), Griffith University Erosion System Template (GUEST) (Ciesiolka et al. 1995), Limburg Soil Erosion Model (LISEM) (De et al. 1998), and Water Erosion Prediction Project (WEPP) (Laen et al. 1991) are the physical process-based models that are also used to estimate soil loss.

Among these models, empirical model RUSLE is found to be useful for estimation of soil erosion rate (Borrelli et al. 2017; Thomas et al. 2018; Terranova et al. 2009; Lu et al. 2004; Nyakatawa et al. 2001; Biesemans et al. 2000). The output from RUSLE was found to be more close to observation (Mondal et al. 2017) and showed lower variability from observation using the fine resolution DEMs. Since the assessment of soil erosion by RUSLE is quite efficient from the prioritization aspect, it becomes more helpful for policymakers to understand the erosion prone area and remedial measures (Wijesundara et al. 2018). The coupling of RUSLE and GIS interface has several advantages and has shown good results to model soil loss (Perovic et al. 2013). Therefore, RUSLE has been successfully applied worldwide to assess soil erosion (Panagos et al. 2019; Koirala et al. 2019; Borrelli et al. 2017; Panagos et al. 2015a, b; Terranova et al. 2009; Lu et al. 2004; Uddin et al. 2016; Waikar et al. 2014), and a limited research has been conducted in the regions, which have complex topography (e.g., river system of Himalayan region).

The major goal of the study was to assess the spatial distribution of soil loss in a humid subtropical trans-boundary river basin. The objectives to fulfill the goal were (i) to assess soil loss by RUSLE model using DEMs of different resolutions; (ii) to

point out the relevance of water retention of soil types in erosion process; (iii) to prioritize erosion zones in the Ghaghara river basin for conservation measures; and (iv) to determine efficiency of hypsometric analysis for recognition of basin's age due to subsequent soil erosion in the basin. With these objectives, an integrated framework was developed for estimation of soil loss.

## 2 Materials and methods

### 2.1 Study area

The Ghaghara river basin is a trans-boundary river also known as Karnali in Nepal (Fig. 1). It originates near Lake Mansarovar (30.60° N, 81.48° E) with a catchment area of 127,950 km<sup>2</sup>. It meets with its tributary Sarda at Brahmaghat in India from where it is known as the Ghaghara river. It joins to the river Ganga at Doriganj situated downstream of Chhapra town, Bihar. The other important tributaries are Sarju, Rapti, and Little Gandak. There are two streams, Seti River and Bheri River, which drain into the Ghaghara river basin in Nepal. The river basin is heterogeneous from source to mouth and has the longest distance river in Nepal (~507 km). The dominant land use/land cover (LULC) type is cropland followed by mixed forest and grassland. The quaternary age sediments are dominant in the basin as Pleistocene age has older alluvium (yellow to brown color), and Holocene age has newer alluvium (gray to black color). The soil types are mostly clay loam, loam, and glacier type. The geomorphology of the Ghaghara river basin contains structural origin, which is high, moderate, and low dissected hills and valleys. In alluvial plain, the Ghaghara river basin shows a meandering pattern with several oxbow lakes and it is a humid subtropical and receives an average annual rainfall of 1041 mm (annual). The temperature distribution is 47 °C (max) in summer to 2 °C (min) in winter. The higher elevation zone is occupied by northeast and northwest, while the lower elevation zone occupies their lower alluvium zone (South-east). It

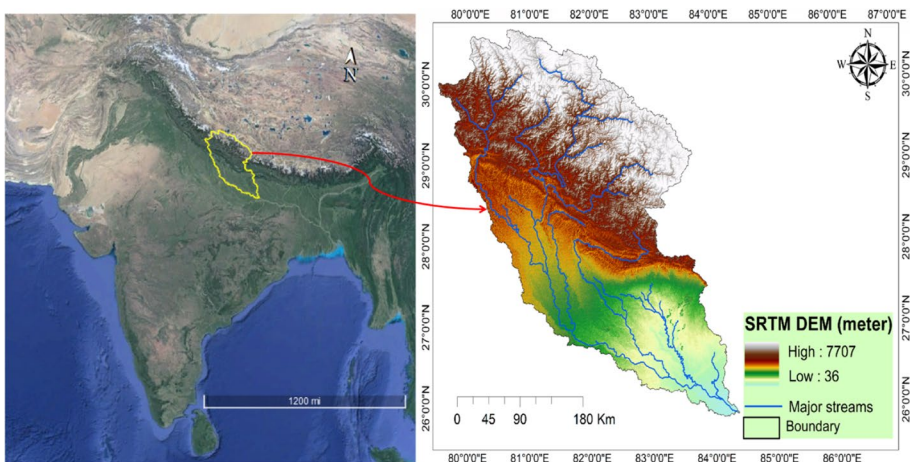


**Fig. 1** Location map of the Ghaghara river basin is showing maximum and minimum elevation with major streams originated near the Mansarovar lake

has a higher discharge than the Ganga before its confluence near Maharajganj, Chhapra district of Bihar. It is a unique river with respect to fluctuation of discharge (very high discharge during monsoon and very low discharge during dry season), high sediment load, and channel instability.

## 2.2 Methodology

The soil erosion from the Ghaghara river basin was calculated using digital elevation models (DEMs), soil, and LULC map. These datasets have been used as input into RUSLE model for estimation of soil loss. The DEM was also used for computation of the basin's morphometric parameters, whereas soil parameters were used to calculate soil water holding capacity. The rainfall data-sets were used for computation of rainfall erosivity. Besides these geomorphic stages of basin, the hypsometric integral and hypsometric curve were estimated using the CalHypso tool available in QGIS. The process of work can be seen in the methodology chart in Fig. 2.

### 2.2.1 Topographic data

DEMs from SRTM (90 m and 30 m), MERIT 90 m, and ALOS 30 m were downloaded from webportal (<http://srtm.csi.cgiar.org/>), ([http://hydro.iis.u-tokyo.ac.jp/~yamada/MERIT\\_DEM/](http://hydro.iis.u-tokyo.ac.jp/~yamada/MERIT_DEM/)) and (<https://www.eorc.jaxa.jp/ALOS/en/aw3d30/data/index.htm>), and

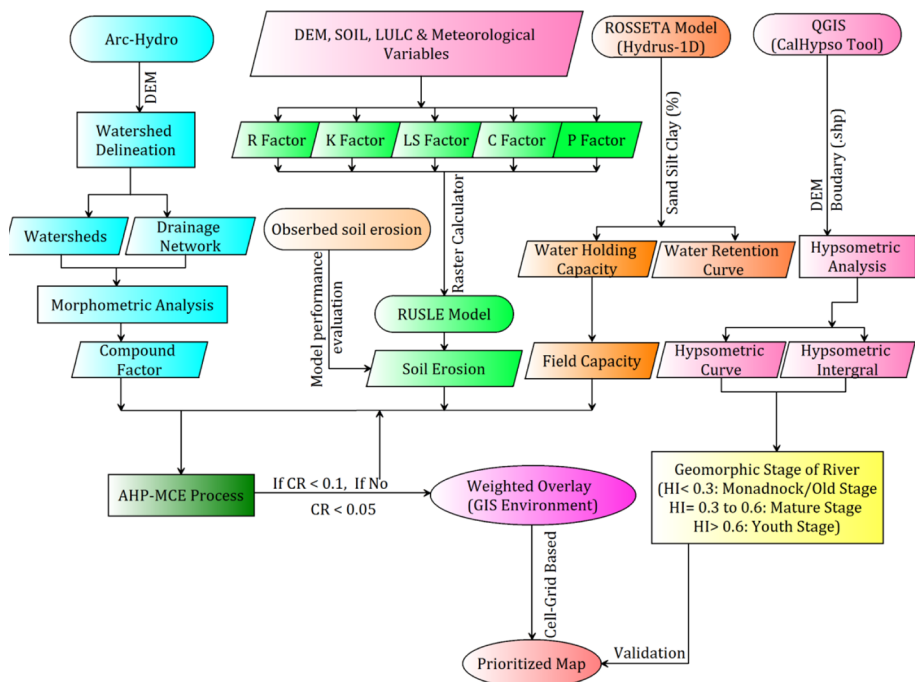


Fig. 2 Adopted methodology for assessment of soil loss in the Ghaghara river basin

the stream delineation process from these four DEMs was performed using D-8 algorithm present in Arc Hydro Tool of ArcGIS. DEM was also used to generate the slope length factor (LS-factor) map for the study.

## 2.2.2 Soil types and meteorological datasets

Soil map of the study region was collected from Food and Agriculture Organization (FAO) soil datasets of 1:50, 00,000 scale (FAO 1977). The classes extracted from soil data are clay\_loam (Bd29-3c-3661), loam (Bd34-2bc-3663), loam (Bd35-1-2b-3664), loam (Be74-2a-3675), loam (Be84-2a-3685), loam (Bk39-2a-3694), loam (Bk40-2a-3695), loam (I-Bh-U-c-3717), loam (I-X-2c-3731), loam (Jc50-2a-3743), loam (Je75-2a-3759), clay\_loam (Rd30-2b-3851), and glacier-6998 (“Appendix- Table 6”). The rainfall was used for calculating the rainfall-runoff erosivity factor (R) to estimate the soil loss by RUSLE model.

## 2.2.3 Land use/land cover (LULC)

The LULC map from MODIS (<https://archive.usgs.gov/archive/>) of 0.5 km resolution was collected and used for the computation of P-factor MODIS of year 2015 has 15 LULC types: water, evergreen needle and broad leaf forest, deciduous needle, and broadleaf forest, mixed forest, shrubland, savanna, grassland, wetlands-mixed, agricultural land, built-up, cropland/woodland mosaic, snow or ice, and barren or sparsely vegetated. The cropland has highest areal extent followed by mixed forest and grassland, while the deciduous needle leaf forest has lowest areal extent in the year 2015 (“Appendix-Table 7”).

## 2.2.4 Estimation of morphometric parameters

The entire region was delineated into 30 sub-basins for detailed and sub-basin level morphometric analysis. The basic, linear, and shape morphometric parameters (Table 1) were estimated using the stream order generated during the delineation of basin. The method used for the ordering of the streams was developed by Strahler order. The numbers of streams (N) of a different order, stream length ( $L_u$ ), area (A), perimeter (P), basin length ( $L_b$ ) are the basic parameters. Strahler (1964) suggested the smallest and un-branched streams are the first-order stream and when two first-order streams confluence, generate second-order stream, and when two second-order streams join, they form third-order and so on. Following the rule suggested by Strahler (1964), when two different order streams join together, the higher order should be counted.

The total length of an individual stream in each order is the stream length ( $L_u$ ) of that order (Horton 1945). The drainage area (A) is the total area where the fluvial generated stream or systems of streams are drained in the corresponding space, and this area provides more detailed information about the basin. The total runoff and sediment load can be easily understood and estimated using the drainage area (A) (Pradhan et al. 2018). Further, basin length ( $L_b$ ) helps to calculate the other linear parameters like form factor, shape factor, and elongation ratio. Ratnam et al. (2005) method was used to calculate the basin length for the study area.

Stream length ratio ( $R_L$ ), bifurcation ratio ( $R_b$ ), drainage density ( $D_d$ ), stream frequency ( $S_f$ ), and length of overland flow ( $L_o$ ) are the linear parameters. These linear parameters

**Table 1** Morphometric parameters, their mathematical expressions and references are presented in table, which are used for assessment of soil erosion in the study area

Parameters	Formula	References
Stream order (U)	Hierarchical rank	Strahler (1964)
Stream length ( $L_u$ )	Length of the stream	Horton (1945)
Stream length ratio ( $R_L$ )	$R_L = L_u / (L_{u-1})$ where $L_{u-1}$ = Total stream length of its next lower order	Horton (1945)
Bifurcation ratio ( $R_b$ )	$R_b = N_u / N_{u+1}$ , where $N_u$ = Number of stream, $N_{u+1}$ = Number of stream of its next order	Schumm (1956)
Drainage density ( $D_d$ )	$D_d = L_u / A$ , where A = Area of study region, $L_u$ = length of stream	Horton (1945)
Stream frequency ( $F_s$ )	$F_s = N_u / A$ , where $N_u$ = Number of stream, A = area of the study region	Horton (1945)
Elongation ratio ( $R_e$ )	$R_e = D / L_b$ , where D = Diameter of a circle having the same area as of the basin, $L_b$ = Basin length	Schumm (1956)
Circulatory ratio ( $R_c$ )	$R_c = 4\pi A / P^2$ , where P = Perimeter of basin, A = area of the study region	Strahler (1964)
Form factor ( $F_f$ )	$F_f = A / L_b^2$ , where $L_b$ = Basin length, A = area of the study region	Horton (1945)
Shape factor ( $B_s$ )	$B_s = L_b^2 / A$ , where $L_b$ = Basin length, A = area of the study region	Horton (1932)
Length of over land flow ( $L_o$ )	$L_o = 0.5 \times D_d$ , where $D_d$ = drainage density	Horton (1945)
Basin length ( $L_b$ )	$L_b = 1.312 \times A^{0.568}$ , where A = area of the study region	Ratnam et al. (2005)
Compactness factor ( $C_c$ )	$C_c = (0.2821 \times P) / A^{0.5}$ , where P = perimeter, A = area of the study region	Horton (1945)

were calculated using the basic parameters information. The  $R_L$  is a dimensionless ratio, which is simply a ratio of stream length, and this method was proposed by Horton (1945). The  $R_b$  is the ratio of stream number, and formula used here to calculate the  $R_b$  is given by Schumm (1956). Horton (1945) described the  $D_d$  ratio of stream length, and area of a sub-basin and  $S_f$  as ratio of stream number and area a sub-basin. Horton (1945) explained the length of overland flow ( $L_o$ ) as one half of the drainage density of the sub-basin.

Furthermore, the shape parameters are form factor ( $F_f$ ), elongation ratio ( $R_e$ ), circularity ratio ( $R_c$ ), shape factor ( $B_s$ ), compactness constant ( $C_c$ ) which have been calculated. The definition of the ( $F_f$ ) was proposed by Horton (1945), which is the ratio of area ( $A$ ) to the square of the basin length. The elongation ratio was estimated using the formula given by Schumm (1956) and is the ratio of diameter of a circle having the same area as of the basin and the basin length.

The circulatory ratio given by Strahler (1964) is the ratio of basin area ( $A$ ) to the square of basin perimeter for which the area is calculated. The shape factor was estimated following the Horton (1932) rule, and it is the ratio of square of basin length ( $L_b$ ) to area ( $A$ ) of that basin. The compactness constant is proposed by Horton (1945) and also expressed by Gravelius (1914) as ratio of basin perimeter ( $P$ ) divided by the circumference of a circle which has the same basin area ( $A$ ). The linear and shape parameters were used to estimate the compound factor and then prioritization of sub-basin.

### 2.2.5 Compound factor and prioritization of sub-basin

The linear and shape parameters of morphometry play an important role to prioritize the basin based on compound factor. The linear parameters are directly concerned with erosion activity, and this means that the higher values of a linear factor in a sub-basin explain the high degree of erosion for that area. However, the shape parameters have the opposite concern to the linear parameters. Therefore, the sub-basin which has a lower value of shape factor that indicates the higher erosion in area. Thus, for our study area rank 1 is given to the sub-basin, which has a higher value of the linear parameters and lower value of the shape parameters, and rank 30 is given to the sub-basin, which has the lowest linear and highest shape factor, and so on. The compound factor has been estimated by the addition of all rank of shape and linear parameters, and after this, we have divided the total sum by the total no. of parameters. Based on results of compound factor, prioritization of sub-basin was performed by giving the first rank to the sub-basin, which has a lower value of the compound factor, and similarly, the last rank is assigned to the sub-basin which has a higher value of compound factor (Maurya et al. 2016).

### 2.2.6 RUSLE model

RUSLE is an advanced form of the USLE developed by Wischmeier and Smith (1978). This model was used at many places to estimate the erosion of the upper surface soil due to rainfall and other factors such as soil and length-slope factor (Pradhan et al. 2018; Panagos et al. 2015a).

The equation 1 of the RUSLE is given as follows:

$$A = R \times K \times LS \times C \times P \quad (1)$$

where A: annual sediment yield ( $t\ ha^{-1}year^{-1}$ ); R: rainfall erosivity factor ( $MJmmha^{-1}\ h^{-1}year^{-1}$ ); K: soil erodibility factor ( $t\ ha\ MJ^{-1}\ mm^{-1}$ ); LS: slope length and steepness factor; C: cover management factor (C); and P: conservation practice factor. LS, C, and P are the dimensions less factor.

The R factor was estimated using the annual rainfall based on Yu and Rosewell (1996) method. The K-factor was calculated using the soil properties and sand, silt, clay, and organic carbon by Sharpley and Williams (1990) formula. The slope length (L) and steepness factor (S) together constitute the topographic factor which was calculated based on Desmet and Govers (1996) in SAGA GIS. The LS-factor was calculated based on DEMs of SRTM 30 m, ALOS 30 m, MERIT 90 m, and SRTM 90 m, respectively. The value of C-factor was assigned by choosing representative values of crop management factor from Tables 5, 10, and 11 given in Wischmeier and Smith (1978). Here, the value of P-factor was selected using LULC map and from the published sources (Liu et al. 2015; Jain et al. 2001; Renard et al. 1996). Finally, all RUSLE factors are multiplied in order to determine soil loss in the Ghaghara river basin. Total four soil erosion rate maps were prepared using the four different LS-factors, which were generated by four different DEMs and keeping the same R-factor, K-factor, C-factor, and P-factor. Further, these RUSLE results were evaluated using the observed data of soil loss in the basin by the Central Water Commission (CWC), New Delhi, India.

## 2.2.7 ROSETTA Model

The ROSETTA from the Hydrus model was used to calculate soil hydraulic properties for the Ghaghara river basin. The water retention curve was prepared using ROSETTA, and this curve describes the water holding capacity of soil under differential pressure head (Maurya et al. 2016). The soils' hydraulic parameters are essential to study water resources. Still, usually, these data are not available on the appropriate scale (Schaap et al. 2001). ROSETTA is commonly used software to achieve the hydraulic parameters of the soil from the sand, silt, and clay proportional values (Pradhan et al. 2018). The ROSETTA model applies the hierarchical pedotransfer functions (PTFs) and a neural network algorithm with bootstrapping (Schaap et al. 2001). The hierarchy in pedotransfer functions (PTFs) allows the ROSETTA model to predict Van Genuchten (1980) water retention curves. The formula (2) for the water retention curve is as follows:

$$\theta_h = \theta_r(\text{residual water content}) + \frac{[\theta_s - \theta_r]}{(1 + (\alpha h)^n)^m} \quad (2)$$

where  $\theta(h)$  is the water content ( $cm^3/cm^3$ ) at soil water pressure head  $h$  (cm),  $\alpha$  is the scaling parameter,  $n$  is the curve shape factor, and  $m = 1 - 1/n$ ;  $\theta_s$  : saturated water content  $\theta_r$  : residual water content

There are 33 kPa and 1500 kPa pressure head (H) defined in the ROSSTEA model to prepare the water retention curve using the sand, silt, and clay value of soil. The 33 kPa indicates the upper limit of water availability by plants known as field capacity, and the 1500 kPa indicates the lower limit of water availability by plants known as a wilting point, respectively (Adhikary et al. 2008). We have estimated field capacity of soil at 33 kPa for all soil types in the study catchment.



## 2.2.8 Multi-Criteria Evaluation (MCE) and weighting assignment

Multi-criteria evaluation (MCE) is a 5 steps pair-wise comparison relation process as (i) pair-wise ranking, (ii) decision matrix, (iii) eigenvalue/vector, (iv) consistency ratio, and (v) priority of criteria. Gupta and Srivastava (2010) explain the MCE, which is AHP based on assigning the weighting of each factor, keeping the view that which parameters are most influencing soil erosion and which parameters have the least importance cause the soil erosion in the basin. In the MCE, which supports the multi-criteria decision making and developed by Saaty (1980), ranking ranges 1 to 9 where 1 indicates less important parameter and 9 refers to the most responsible factor for soil erosion (Saaty et al. 1980; Srivastava et al. 2012). The ratio scales were generated using paired comparisons of criteria in AHP with some inconsistencies in judgments. Then, priorities (weightings) of criteria and consistency ratios are calculated (Goepel et al. 2018). The priorities (weightings) of the criteria are derived using the principal eigenvector ( $e$ ) of the matrix  $M$  (3), as follows:

$$M_e = \lambda_{\max} \times e \quad (3)$$

According to Saaty (1980), the value of consistency ratio ( $CR \leq 0.1$ ). The CR and CI can be estimated using the following formula given below (4) and (5):

$$CR = \frac{CI}{RI} \quad (4)$$

$$CI = \frac{(\lambda_{\max} - n)}{(n - 1)} \quad (5)$$

where  $\lambda_{\max}$  = largest eigenvalue and  $e$  = principle eigenvector

$$CI = (\text{Consistency index}), RI = (\text{Random Inconsistency})$$

where  $n$  is the number of variables.

## 2.2.9 Final prioritized map

Further, results from field capacity (water holding capacity), compound factor, and RUSLE were used to generate a prioritized map for the distribution of erosion patterns in the basin. The prioritized map was prepared using the above three factors and the weighing overlay method on the GIS platform. Final erosion map was classified into five zones to the erosion variability in the region as very low, low, moderate, high, and very high zone in respect of erosion. Although four RUSLE maps were prepared from the four different LS-factors (from four different DEMs), final prioritized map of soil erosion was prepared using the RUSLE results (SRTM 30 m DEM), which was more closed to observed data in the basin.

## 2.2.10 Hypsometry of sub-basins

The hypsometry simply relates to the measurement of land elevation which aims to develop a dimensionless ratio of cross section area of the basin to its elevation (Dowling et al. 1998). Strahler (1952) stated that the hypsometric analysis could help to identify the erosion status at a different level. The hypsometric integral (HI) and hypsometric curve (HC)

are the two special outcomes of the hypsometry (Singh and Singh 2018), which serves as an indicator of sub-basin condition (Ritter et al. 2002). The HI and HC have calculated using the DEM with QGIS (Quantum GIS 2019) using the CalHypso extension for the hypsometry at basin and sub-basin level. The basic method behind the calculation of hypsometric integral (HI) is given by Pike and Wilson (1971), which is simply an elevation-relief ratio. The following relationship is as given below Eqn. (6):

$$HI = (Elev_{\text{mean}} - Elev_{\text{min}}) / (Elev_{\text{max}} - Elev_{\text{min}}) \quad (6)$$

where  $Elev_{\text{mean}}$ : weighted mean elevation of the sub-basin;  $Elev_{\text{max}}$ : Maximum elevation within the sub-basin; and  $Elev_{\text{min}}$ : Minimum elevation within the sub-basin.

### 3 Results

Among these soil classes, loam (Be84-2a-3685) is dominant soil type with 41,275 km<sup>2</sup> (32.12%) followed by loam (I-Bh-U-c-3717) and loam (Bd34-2bc-3663). The lowest coverage area soil is loam (Be74-2a-3675), having 27.56 km<sup>2</sup> of total area. The dominant land use/land cover is cropland and illustrated in Fig. 3.

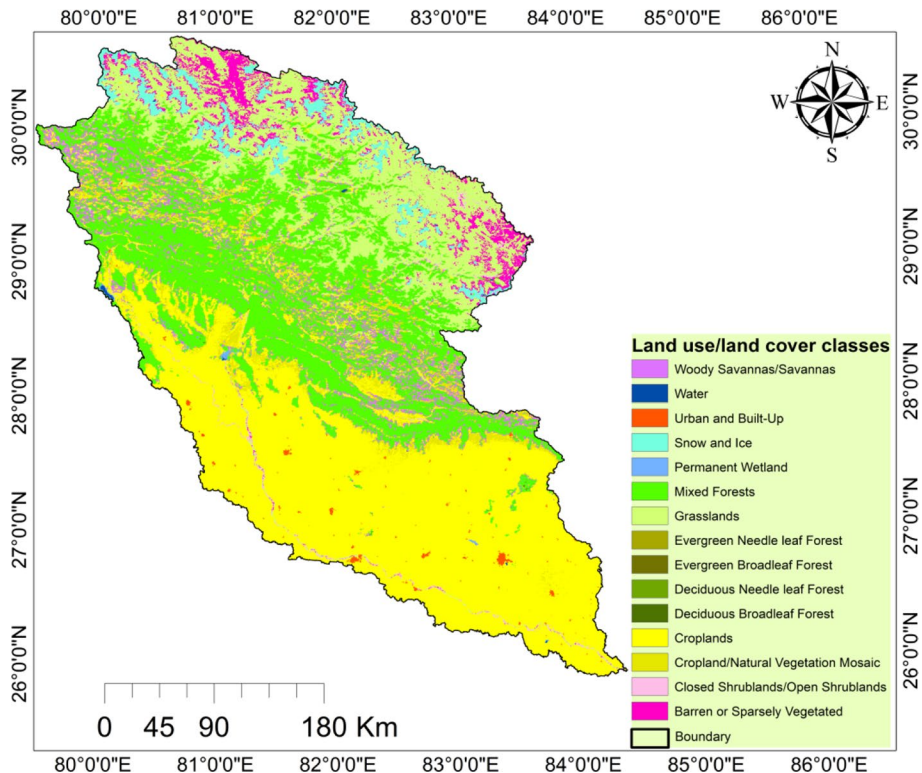


**Fig. 3** Land use/land cover (LULC) map is showing a class distribution in the study area

### 3.1 Morphometric analysis and prioritization of sub-basin

The results of morphometric analysis showed total fifth order of streams (first order to fifth order) for quantitative evaluation of basin and also to interpret the morphodynamic characteristics (“Appendix-Table 8”). The highest number of streams (465) was occupied by the first-order stream, while the lowest number (46) by the fifth-order stream. Among the sub-basin, a maximum of 64 streams laid in the sub-basin 18, while the minimum 7 streams were laid in the sub-basin 30. The results showed that first-order streams were of a smaller length stream, but their total length was greater than other higher-order streams for each sub-basin. The sub-basin 18 was occupied by the higher stream length (1186.93 km), while 30 sub-basins occupied by the lower stream length (117.56 km). The sub-basin no. 18 had the highest drainage area (9240.95 km<sup>2</sup> km<sup>2</sup>), while the sub-basin 30 had the lowest (958.71 km<sup>2</sup>) drainage area. The highest (1240 km) and lowest (349.76 km) value of perimeter was found in sub-basin 18 and sub-basin 30, respectively. Similarly, the basin length ( $L_b$ ) ( $L_b$ ) was highest (234.67 km) for the sub-basin 18 and lowest (64.79 km) for sub-basin 30.

The  $R_L$  value for the basin was ranged from 5.513 (max.) to 0.524 (min.) for sub-basins 25 and 1, respectively, whereas value of  $R_b$  ranged from 4.392 (max) to 1.205 (min) for the

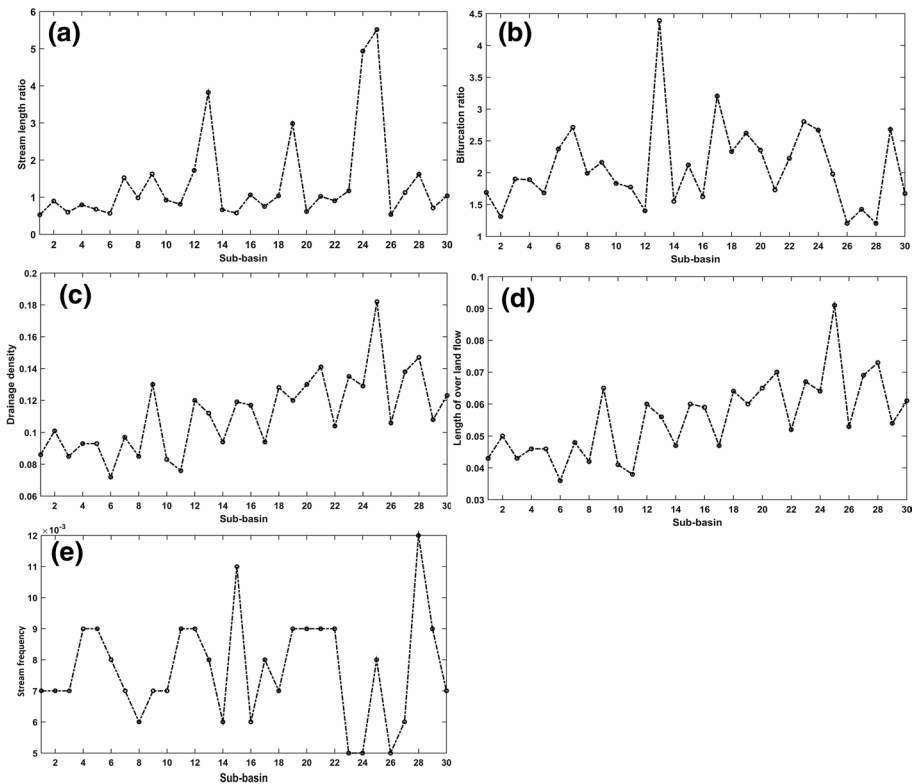


**Fig. 4** a Sub-basin-wise stream length ratio in the Ghaghara river basin, b sub-basin-wise bifurcation ratio, c sub-basin-wise drainage density, d sub-basin-wise length of over land flow, and e sub-basin-wise stream frequency in the Ghaghara river basin

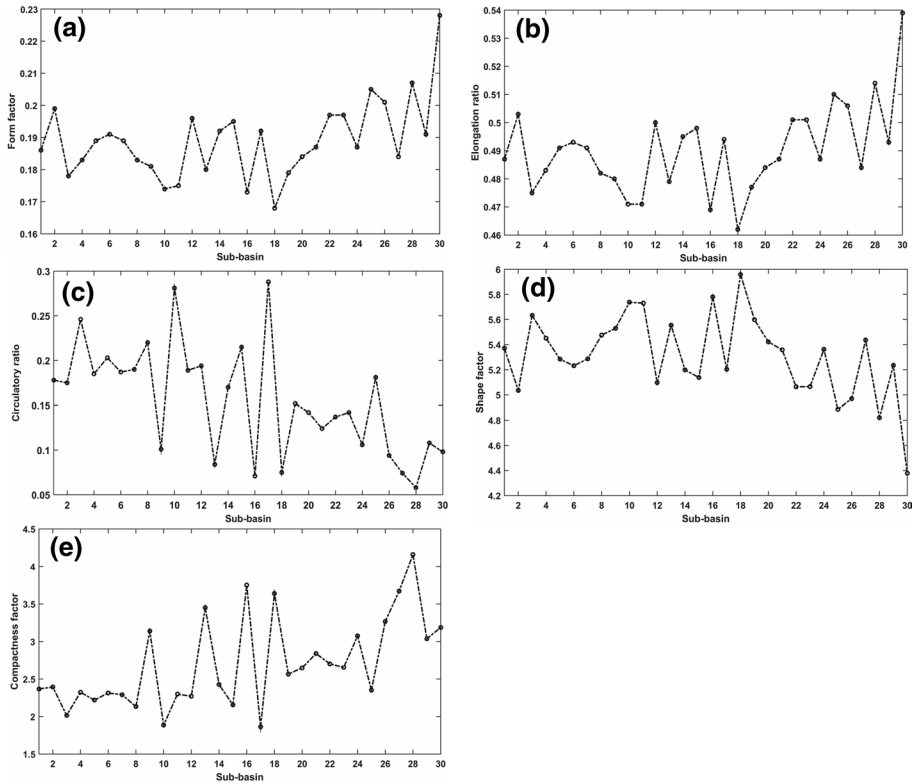


**Fig. 5** **a** Sub-basin-wise form factor in the Ghaghara river basin, **b** sub-basin-wise elongation ratio, **c** sub-basin-wise circulatory ratio, **d** sub-basin-wise shape factor, and **e** sub-basin-wise compactness factor in the Ghaghara river basin

sub-basins 13 and 28, respectively (“Appendix-Table 9”; Fig. 4 a-e). The overall  $R_b$  for the basin was 1.821. The other linear parameters as  $D_d$  were varied over 0.182 (max) to 0.072 (min) for sub-basins 25 and 6, respectively. The value of  $L_o$  was max (0.091) for sub-basin 25 and min (0.036) for sub-basin no. 6. The  $S_f$  showed maximum value (0.012) for the sub-basin 28 and minimum value (0.005) for sub-basins 23 and 24.

The results of shape morphometric parameters showed that form factor ( $F_f$ ) was varied from 0.228 (maximum) to 0.168 (minimum) for sub-basins 30 and 18, while elongation ratio ( $R_e$ ) was 0.539 (maximum) to 0.462 (minimum) for the sub-basins 30 and 18 (Fig. 5 a, b, c, d and e). The circulatory ratio ( $R_c$ ) was ranged from 0.288 (maximum) to 0.058 (minimum) for sub-basins 17 and 28, while the shape factor was from 5.959 (maximum) to 4.379 (minimum) for the sub-basins 18 and 30. The compactness factor ( $C_c$ ) for the study area varied from 4.158 (maximum) to 1.864 (minimum) for the sub-basins 28 and 17. The prioritization for the Ghaghara river basin was done, and sub-basin 19 was assigned as first rank following sub-basins 13 and 9, while the last rank was assigned to sub-basin 26 (“Appendix-Table 10”).

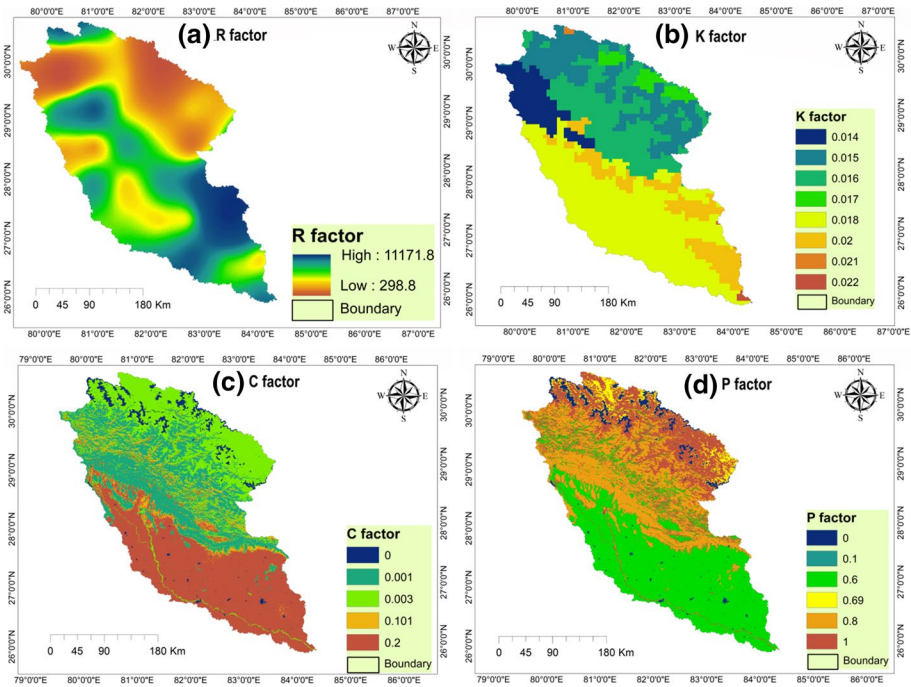


**Fig. 6** a Rainfall-runoff erosivity map (R factor), b soil erodibility factor map (K-factor), c cover management factor map (C-factor), and d support practice factor map (P-factor)

### 3.2 RUSLE

The rainfall-erosivity factor (R) for the Ghaghara river basin was ranged from 298.8 (north-east and north-west part of the basin) to the 11,171.8 MJmmha<sup>-1</sup> h<sup>-1</sup>y<sup>-1</sup> (middle and lower part of the basin) (Fig. 6a). The soil erodibility factor (K) ranges between 0 and 1, where K-factor near to 0 means less susceptibility for erosion and K-factor near to 1 is represented higher susceptibility for soil erosion. The value of K-factor estimated for the basin ranges from 0.014 to 0.022 (takhha<sup>-1</sup> MJ<sup>-1</sup> mm<sup>-1</sup>) (Fig. 6b). The upper portion of the basin was occupied by the lower K-factor, while the middle and central portion was occupied by the higher erodibility factor in the basin. The cover management factor (C-factor) in the Ghaghara river basin ranged from 0 to 0.2. The higher value of C-factor was found in central and lower region of the basin, while the upper part of the basin was occupied by lower value of C-factor in the basin (Fig. 6c). The P-factor value in the Ghaghara river basin ranged from 0 to 1 (Fig. 6d). The moderate P-factor value occupied the lower central portion of the basin. The upper portion was mostly shown the higher value of P-factor nearly 1 or close to 1, but some portion of the upper basin was also occupied by the lower or zero P-factor value.

The value of LS-factor for SRTM 30 DEM varied over 0.03 to 100.66, and for ALOS 30 m DEM, it was 0.03 to 102.54 in the basin (Fig. 7a, b). The LS-factor for MERIT 90 m DEM was 0.03 to 33.34, while for SRTM 90 m DEM, it varied over 0.03 to 128 in the basin (Fig. 7c, d). The upper portion of basin augmented the higher value of LS-factor,

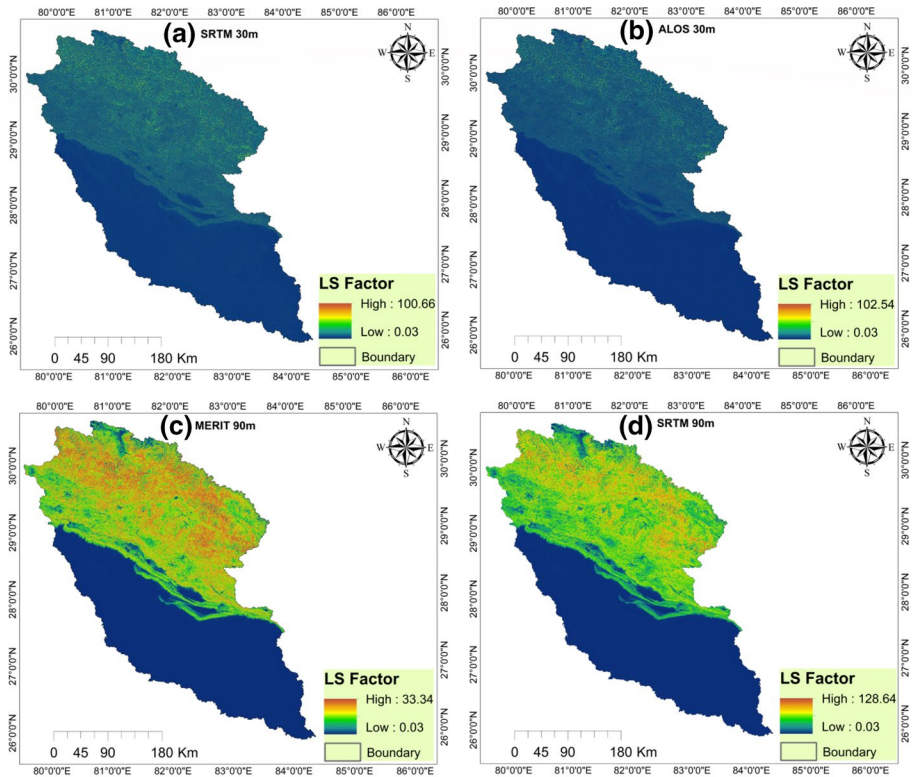


**Fig. 7** Topographic factor maps (LS-factor) are showing high and low value of LS-factors for **a** SRTM 30 m DEM, **b** ALOS 30 m DEM, **c** MERIT 90 m DEM, and **d** SRTM 90 m DEM in the study area

while the lowest value of LS-factor laid in the middle and downstream portion of basin for all four DEMs.

### 3.3 Soil erosion rate and model performance

The annual rate of soil erosion was estimated by multiplication of five RUSLE factors (for different DEMs), which had shown soil loss in the basin. The erosion rates were 21.39, 18.31, 4.35, and 4.64 ton/ha/year for SRTM 30 m, ALOS 30 m, MERIT 90 m, and SRTM 90 m, respectively (Table 2). We had evaluated the RUSLE results for all DEMs using observed data, and the percentage of changes in soil erosion amount from observed were 13.98%, 26.38%, 82.51%, and 81.34%, respectively, for SRTM 30 m, ALOS 30 m, MERIT 90 m, and SRTM 90 m. The results showed that among the annual soil erosion rate estimated using different DEM, the RUSLE soil erosion rate of SRTM 30 m was more closed (13.98%) to observed data, followed by the soil erosion rate of ALOS 30 m (26.38%). The soil erosion rate by 90 m DEMs showed the poor results, whereas soil erosion from fine resolution DEM was closer to observed data.

**Table 2** Annual rate of soil erosion statistics obtained from four different DEMs

DEM type and resolution (m)	Erosion rate min. (ton/ha/year)	Erosion rate max. (ton/ha/year)	Erosion rate std. (ton/ha/year)	Erosion rate mean (ton/ha/year)	Erosion amount (ton/year)	Observed amount (ton/year)	Difference (ton/year)	Difference (%)
SRTM 30	0.3	125.1	57.93	21.39	264,345,577.1	307,363,300	43,017,723	13.98
ALOS 30	0.1	107.97	68.28	18.31	226,281,791.3	307,363,300	81,081,509	26.38
MERIT 90	0.05	67.13	17.71	4.35	53,758,918.2	307,363,300	253,604,382	82.51
SRTM 90	0.03	66.9	17.13	4.64	57,342,846.08	307,363,300	250,020,454	81.34

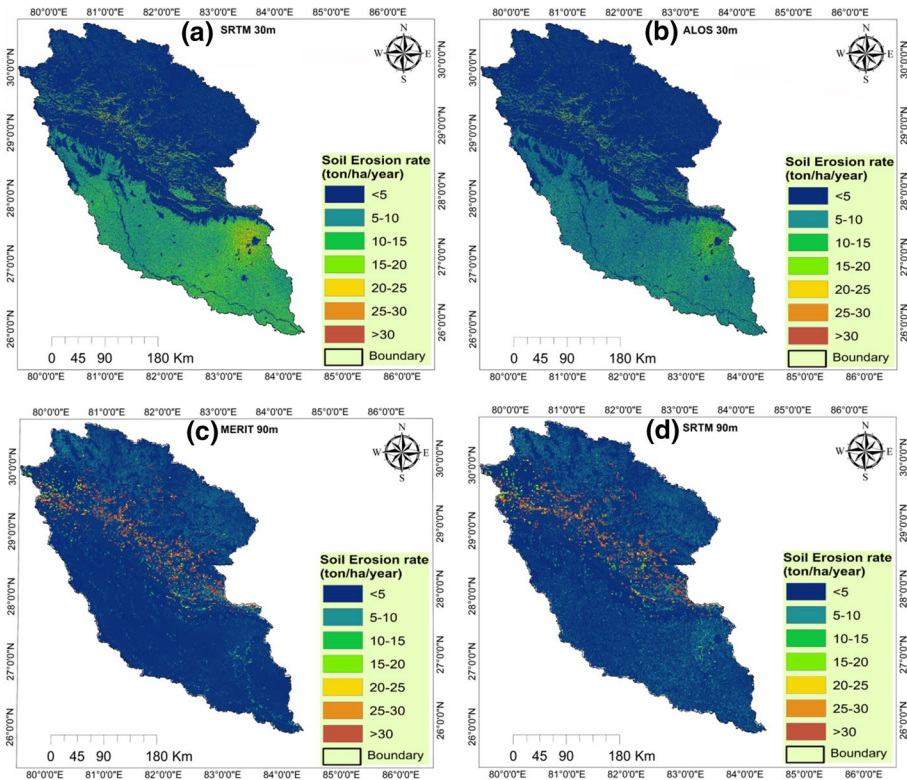


**Fig. 8** The estimated soil erosion rate (ton/ha/year) using RUSLE for **a** SRTM 30 m DEM, **b** ALOS 30 m DEM, **c** MERIT 90 m DEM, and **d** SRTM 90 m DEM is showing the distribution pattern of soil erosion rate in the study area

### 3.4 Spatial variation in soil erosion rate

We had categorized the soil erosion rate into seven different ranges for better understating about the variation of the soil loss in the basin. These seven soil erosion categories were <5, 5–10, 10–15, 15–20, 20–25, 25–30 and >30 ton/ha/year for four different soil erosion rate maps (Fig. 8 a, b, c and d). Overall, the category <5 ton/ha/year was maximally observed in all maps of soil erosion rate for all the DEMs and this category covered the greater upper portion of the basin for SRTM 30 m and ALOS 30 m DEMs. The category 5–10 ton/ha/year was mostly covered the lower middle portion for erosion rate map of ALOS 30 m and SRTM 30 m DEMs. The category 10–15 and 15–20 ton/ha/year covered the low portion for all DEMs. The higher erosion rate categories (20–25, 25–30 and >30 ton/ha/year) were occupied by the south-east and the middle portion for SRTM 30 m and ALOS 30 m DEMs while middle portions for MERIT 90 m and SRTM 90 m DEMs.



**Table 3** Water holding capacity based on soil types in the Ghaghara river basin

Sr. No	Soil texture	Soil types	Water holding capacity (m <sup>3</sup> /m <sup>3</sup> )
1	CLAY_LOAM	Bd29-3c-3661	0.284
2	LOAM	Bd34-2bc-3663	0.240
3	LOAM	Bd35-1-2b-3664	0.222
4	LOAM	Be74-2a-3675	0.239
5	LOAM	Bd84-2a-3685	0.242
6	LOAM	Bk39-2a-3694	0.246
7	LOAM	Bk40-2a-3695	0.244
8	LOAM	Bh-U-c-3717	0.246
9	LOAM	I-X-2c-3731	0.232
10	LOAM-6998	Jc50-2a-3743	0.251
11	LOAM	je75-2a-3759	0.244
12	CLAY_LOAM	Rd30-2b-3851	0.257
13	UWB	GLACIER-6998	0.220

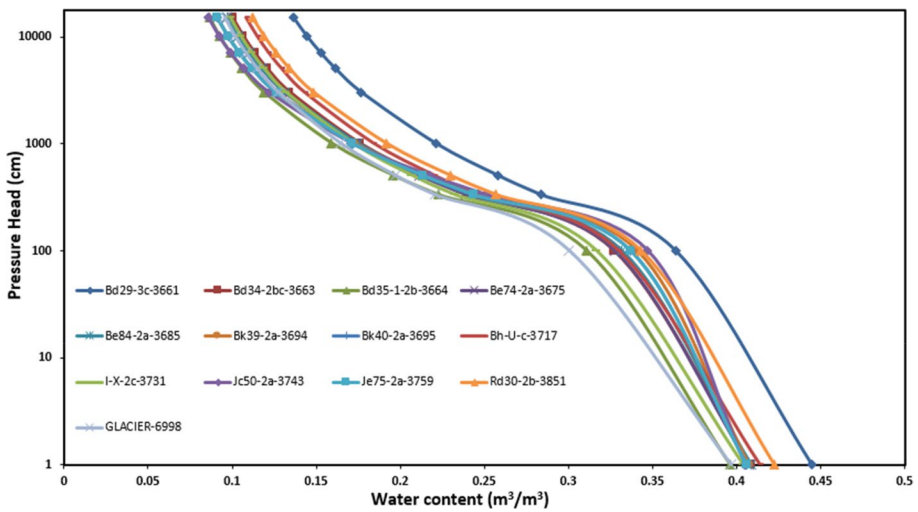


**Fig. 9** A schematic diagram of water retention curve for different soil types in the Ghaghara river basin

**Table 4** Pair-wise comparison matrix by MCE-AHP method for weighting four factors

Parameters	RUSLE	Compound factor	Field capacity	Priority (normalized weight)	Rank	CR
RUSLE	1	4	8	71.6%	1	0.02
Compound Factor	0.25	1	3	20.5%	2	
Field Capacity	0.125	0.33	1	7.8%	3	

### 3.5 Soil hydraulic parameters

Table 3 shows water holding capacity of soil types in the Ghaghara river basin. The soil clay\_loam (Bd29-3c-3661) shows the highest value of field capacity ( $0.284 \text{ cm}^3/\text{cm}^3$ ), while the clay\_loam (Rd30-2b-3851) has  $0.257 \text{ cm}^3/\text{cm}^3$  and loam (Jc50-2a-3743) has ( $0.251 \text{ cm}^3/\text{cm}^3$ ), respectively. The other soil types showed moderate to lower capacity, while the lowest rank was accounted by glacier-6998 ( $0.22 \text{ cm}^3/\text{cm}^3$ ) (Fig. 9).

### 3.6 Multi-criteria evaluation (MCE) and final prioritized map

For the Ghaghara river basin, to use the MCE-based methodology, three factors (compound factor from morphometric analysis, erosion of soil from RUSLE, and filed capacity (ROSETTA) from the soil had been constituted. MCE was applied to these factors to schedule soil erosion prone zone in the entire basin and so that subsequent conservation measures can be applied. Following, the procedure of AHP based MCE, the estimated consistency ratio was 0.02, which was less than 0.1 (Table 4) and according to Saaty (1980) it is considered as good and acceptable. The above three factors were explained by their decision matrix and priority criteria (weighting) using the MCE. The highest weighting was given to RUSLE model (71.6%) followed by compound factor (20.5%) and field capacity

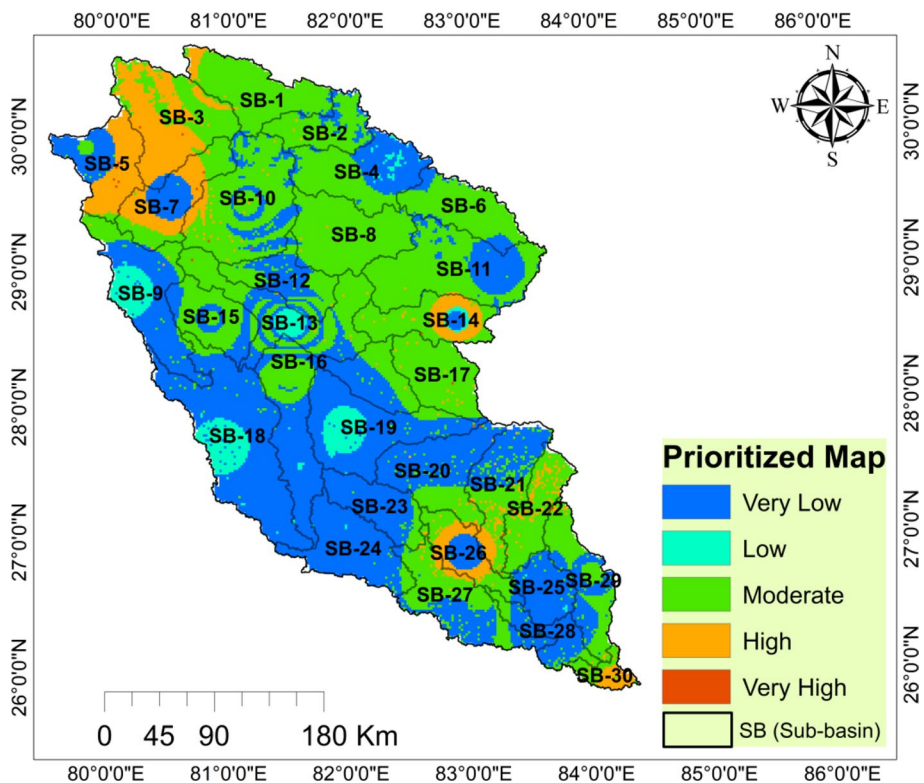


**Fig. 10** Prioritized map is showing areas which are needed interventions for conservation practices in the Ghaghara river basin

(7.8%) which had 2nd and 3rd rank, respectively. The result of the final prioritized map (Fig. 10) showed that erosion activity in the middle part of the basin ranged from high to very high (SB-3, SB-5, SB-7, SB-14, SB-26, and SB-30).

The northern upper (SB-1, SB-2, SB-4, SB-6, SB-8, SB-10, SB-11, SB-15, SB-17) and lower portion (SB-21, SB-22, SB-27) show moderate erosion. The SB-9, SB-16, SB-18, SB-19, SB-20, SB-23, SB-24 show low to very low erosion in the basin. The high erosion zone captured the 9.30%, while moderate erosion zone occupies the 46.72% area of the basin (Table 5).

### 3.7 Hypsometric analysis

Hypsometric parameters (HI and HC) of the Ghaghara river basin were acquired at sub-basin level for the detailed analysis of mass movement (erosion) happening in the basin (Figs. 11, 12). The HI values are categorised into 3 zones for easy identification of the erosion prone zone, and these zones are as follows 0 to 0.3, 0.3 to 0.6, and above 0.6, respectively. If the HI value of the sub-basin is 0.3, it means that 30% of original rock mass still exist in that sub-basin. The HI value of the Ghaghara river basin ranges from 0.032 (min) for the sub-basin number 22 to 0.664 (max) for the sub-basin number 28. The rest of the sub-basins (almost 50%) has value in between 0.3 and 0.6, while others are below the 0.3 and few are above the 0.6 level.

## 4 Discussion

The relation of master streams with their joining tributaries is the drainage system, which shows the topography effect on streams (Strahler 1964). The Ghaghara river basin occupies a more undulating structure from Himalayan chains (upper confluences) to Indo-Gangetic plain (downstream), resulting from different drainage patterns. The upper parts have a trellis pattern, which is a rectangular type (northern and north-east portion), while lower parts consume dendritic and sub-dendritic types. Strahler (1964) has explained the method for ordering streams based on hierarchical ranking. For the Ghaghara river basin, total fifth order of the streams was generated and stream order is inversely proportional to the stream length (Singh and Awasthi 2011). This inverse relation between stream order and stream length is indicator of variation in lithology, moderately steeper slopping pattern and high altitude flowing streams (Singh et al. 2013). Sethupathi et al. (2011) describe the role of stream length in recognizing hydrologic properties (permeability) of rock. Small streams that are large in number follow the less permeable path, while the longer streams of smaller counts follow a more permeable zone. Waikar et al. (2014) explain the role of stream length for revealing surface runoff as small length streams are characterized in slopping area and therefore finer texture, while the larger length streams are indicative of plainer zone. This is also happening in the Ghaghara river basin where larger length streams are maximally dominated in the plain area (lower and middle portion of the basin). The relative capacity of a rock to pass the fluid, discharge, and erosion condition in a basin can also be estimated by taking the ratio of stream length as suggested by Horton (1945) and which is stream length ratio ( $R_L$ ). In the Ghaghara basin, sub-basin 25 has the highest  $R_L$  value, which is

supported by permeable zone (almost sandy area) and gentler gradient than the sub-basin 1, which has the lowest  $R_L$  value and depicts the opposite condition of sub-basin 25.

The above variation in the topographic condition due to  $R_L$  in basin is also supported by Vittala et al. (2004). There are basically two types of bifurcation ratio ( $R_b$ ) as one is low value and another is high value  $R_b$ . The low value  $R_b$  indicates those drainages which are not affected by the geologic constraints, while the high value  $R_b$  is primarily influenced by geologic constraints. Gajbhiye et al. (2014) stated that higher values of  $R_b$  is supported steeply sloping surface with narrow confined valley, therefore, higher chances of more runoff and less recharge in that area. In the Ghaghara river basin, sub-basins 13 and 17 have higher value of  $R_b$ , and these sub-basins are confined to the north-eastern part of the basin proving steeply sloping surface with a narrow confined valley.

Nag and Chakraborty (2003) stated that low  $R_b$  has characteristics of less structural disturbances in that area and lower value  $R_b$  is confined to the lower part of the Ghaghara river basin where drainages are not structurally distorted, yet they are flowing in plain of maturity. The lower part of the basin is permeable and have soft strata therefore a good chance to percolate/infiltrate the surface water to ground-water. The  $D_d$  most vital linear parameters depict the quantitative measure of average length of stream in a particular sub-basin or for the whole area. The lithological properties in terms of porosity and permeability of earth material can also be recognized using  $D_d$  therefore good in decision making for artificial recharge site. The low  $D_d$  area is generally occupied by highly registrant track, and dense vegetation (Nag 1998), and these areas in the Ghaghara river basin are captured by hilly/registrant tracks and middle part having characteristics of dense vegetation. Whereas high value  $D_d$  is found in basin where surface materials are weak and dominantly occupied by sparse vegetation cover.

The vegetation pattern and hydrologic properties of soil (permeability) have a big role in deciding surface runoff and therefore directly decide the density of drainages in that area (Dash et al. 2019). Yadav et al. (2020) also supported above that low  $D_d$  has coarse drainage, while high  $D_d$  has fine drainage texture. Moglen et al. (1998) stated that  $L_o$  is inversely related to  $D_d$ , and important linear parameter governs the hydrologic and physiographic characteristics of a drainage basin. Rama (2014) pointed out that lower  $L_o$  indicated quicker runoff process and vice versa. Here, for the Ghaghara river basin  $L_o$  varies from 0.036 to 0.091 with a mean value of 0.055, whereas upper tracks have lower value, while lower parts have a higher value.

The sub-basins in the Ghaghara river basin, those have a lower  $L_o$  laid in the hilly mountains region where faster runoff carries water from upstream to low lying area. Therefore, sub-basin those have higher value of  $L_o$  gets a chance to accommodate the more water for flooding during intense rainfall period and this is the main characteristics of lower part of the Ghaghara river basin, which causes flooding and erosion in the basin. However, the situation becomes the opposite during the dry period. The sub-basins 4, 5, 11, 15, and 28 have a higher  $S_f$  value, while other sub-basins have low to medium range.

The high  $S_f$  is the characteristics of impermeable subsurface lithology and high relief, while other hydrological properties like infiltration capacity and percolation also help to decide the  $S_f$  of the region. The sub-basins that are occupied by the highest value of  $S_f$  and impermeable lithology in the basin generally produce faster runoff. This faster runoff originates the floods downstream of the basin, and during the rainfall period, the downstream parts of the Ghaghara river basin, especially the Bahraich, Faizabad, Basti, Ambedkar Nagar, and Azamgarh, are inundated with the muddy water. One of the serious impacts of the flooding in the Ghaghara river basin is siltation, which is a complex environmental problem than landslides in the upper part of the basin. Therefore, it is a subject of keen

interest to mitigate the hazard of flooding in cities/villages situated in plainer area where the Ghaghara river comes to mature stage and the chances of flooding and lateral meandering become more dangerous than to down-cutting the basin.

The form factor ( $F_f$ ) is one of the important shape parameters of morphometry, which defines whether the basin is circular or elongated. There is a threshold value 0.78 for deciding the basin to be elongated (if  $F_f < 0.78$ ) or circular shape (if  $F_f > 0.78$ ) (Kumar et al. 2018a), and since  $F_f$  for the Ghaghara river basin is always less than 0.78, therefore, the basin is elongated in shape.

The lower part of the basin, especially sub-basins 25, 26, 28, and 30, has a higher value form factor than the upper part of the basin. Therefore, the sub-basin which has high form factor will report high intensity (peak flow) within a short time, whereas more elongated sub-basins will show lower peak (low flow) of longer time. The factor which influences peak flow and low flow in a basin is basin length ( $L_b$ ), as higher basin length reduces the peak discharge and vice-versa (Rao 2016). Therefore, this elongated sub-basin can be easily managed than a circular sub-basin. The elongation ratio ( $R_e$ ) characterized by the shape of the basin varies from 0.6 to 1.0 in the variability of climatic and geologic setup. The value of  $R_e$  varies from 0 (in highly elongated shape) to unity 1.0 (in a circular shape). The value close to 1.0 depicts low relief, whereas  $R_e$  close to 0.6–0.8 is usually associated with high relief (Strahler 1964). The infiltration capacity of the basin can be checked by the elongation ratio as high  $R_e$  indicates high infiltration capacity, and in the Ghaghara river basin, the higher values are close to sub-basin 28 and 30 where the subsurface material (alluvium) is more permeable therefore higher infiltration capacity.

Reddy et al. (2004) stated about  $R_e$  that areas with lower value are found in the zones which have a higher susceptibility to erosion and sediment load, and these areas are dominated in the low stream and upper stream of the Ghaghara river basin. The appraisal of flood prone areas can be easily performed using the shape morphometric parameter such as circulatory ratio ( $R_c$ ) as the flood concerning parameters like stream length, and its frequency, geological structures, and climate, etc., have great control on  $R_c$ . The higher  $R_c$  causes chance of flooding during peak rainfall condition at outlet point of their sub-basins as this outlet becomes inlets for lower  $R_c$  sub-basin in the downstream part of river basin. The same is true for the Ghaghara river basin as the downstream sub-basins have lower  $R_c$  and receives more water from the upper part of the sub-basin having the higher  $R_c$  value.

Bali et al. (2012) reported the range of  $R_c$  from 0 to 1 and explain morphological stage using this range as lower value of  $R_c$  suggests young/mature stage of the river, while higher value indicates the old stage. For the Ghaghara river basin, the circulatory ratio always closer to the lower circulatory ratio, this suggests that the basin is in young to mature stage. The mean  $R_c$  value is 0.134, which is always less than unity and shows that the shape of the basin is not in a circular pattern, and  $R_e$  and  $R_c$  both have confirmed that the Ghaghara river basin has an elongated shape of the basin.

The shape factor ( $B_s$ ) which is inversely related to the form factor ( $F_f$ ) defines shape irregularity of a sub-basin. The upper and middle sub-basins have higher shape factors, while the downstream sub-basin has a lower value.

Shape factor helps to quantify the head (highest) discharge at the pour point of the basin. As a tributary pattern of a circular-shaped basin is more compactly organized than an elongated-shaped basin having the same area and tributary flow joins to mainstream at roughly the same time, therefore, peak discharge will arrive faster at the outlet of circular basin. Thus, outlet gains the higher flood within a shorter duration. Choubey and Ramola (1997) described that the shape morphometric parameters have an inverse relation to the soil erosion; therefore, the compactness factor ( $C_c$ ) should show the opposite trend to soil

erosion, and it can be concluded that the lower the value of  $C_c$  depicts, higher erosion in that area and vice-versa. The results of compactness factor show that the sub-basins are having a lower value of  $C_c$  following the high to moderate erosion in that area and these sub-basins are situated in the upper portion.

The results of hypsometric analysis also validate the results of  $C_c$  as the upper stream sub-basins are in young to mature stage of the river, and hence, more erosion might be in process. At the same time, the middle and downstream sub-basins occupy the higher value of  $C_c$  in comparison with the upper portion of the basin and, therefore, lower erosion comparison to upstream. Since it has an inverse relationship to elongation ratio, consequently, the downstream sub-basins are more elongated. Gravelius (1914) states that if the  $C_c$  value is unity, then the basin will be perfectly circular, and for the Ghaghara river sub-basins, the value of  $C_c$  is greater than unity; therefore, it is an elongated river basin.

The compound factor and prioritization of sub-basin help to know the sub-basin susceptibility to loss of soil in the Ghaghara river basin. It is important to manage the whole basin at once step; therefore, the prioritization help to implement the conservation practices according to the sub-basin condition. Gajbhiye et al. (2014) also stated that the prioritization of sub-basin based on the ranking of sub-basins are needed for the conservation practices. The low prioritized sub-basin demands higher conservation practices (Pradhan et al. 2018) and vice-versa. The results of the compound factor showed that for the Ghaghara river basin, sub-basin no. 19 (rank 1) is more prioritized, followed by sub-basin no. 13 and 9.

The hydraulic properties of soil help to understand the erosion condition of that area, and therefore, the field capacity of the soil was estimated at different pressure heads for the Ghaghara river basin. The water retention curve depicts that soil clay\_loam (Bd29-3c-3661) has more field capacity which means that this soil will retain and accumulate more water than other soil types, and therefore it will cause a severe erosion during high peak flow. Similar conditions will be followed by the clay loam (Rd30-2b-3851) and loams (I-Bh-U-c-3717 & Jc50-2a-3743) respectively. The soil erosion by RUSLE for all DEMs showed that upper middle and lower (south-east) portions of the basin have a high contribution to soil erosion.

It can be concluded that higher erosion zones are those areas that occupy their position mostly in hilly terrain and where headward and deep erosion process is mostly activated due to their natural topography. Mahapatra (2005) also supported the above argument that hilly terrain areas are characterized by headward and vertical erosion due to the high energy in streams. We have used outcome of RUSLE, compound factor, and water holding capacity (field capacity) to understand erosion pattern in the entire basin as erosion process is very complex and constitutes the role of various factors. Therefore, we have followed MCE-based AHP procedure in order to include the weightage of each factor. The meaning of weightage here indicated the efficiency of parameters to depict soil erosion. The RUSLE model has the highest weightage, followed by the compound factor. The lowest weightage was assigned by field capacity.

The final prioritized map was developed by overlay analysis and had been classified in to five zones to understand soil erosion in the entire basin. The final prioritized map of soil erosion shows that 9.30% of the basin falls under high erosion categories. The areas under low to very low erosion are contributing 40.41 to 3.51%, respectively, in middle and lower parts of the basin where the basin is almost in the monadnock stage (old). The percentage of moderate erosion is 46.72% in the lower, upper, and some middle parts of the basin. For more illustration of the variation of soil erosion in the basin, the total seven categories were generated and results depict the soil erosion rate < 5 ton/ha/year is covering the major portion of the basin for all DEMs. The results of soil erosion for all four DEMs depict that the finer resolution DEMs are predicting the good results and more close to observed data. Here,

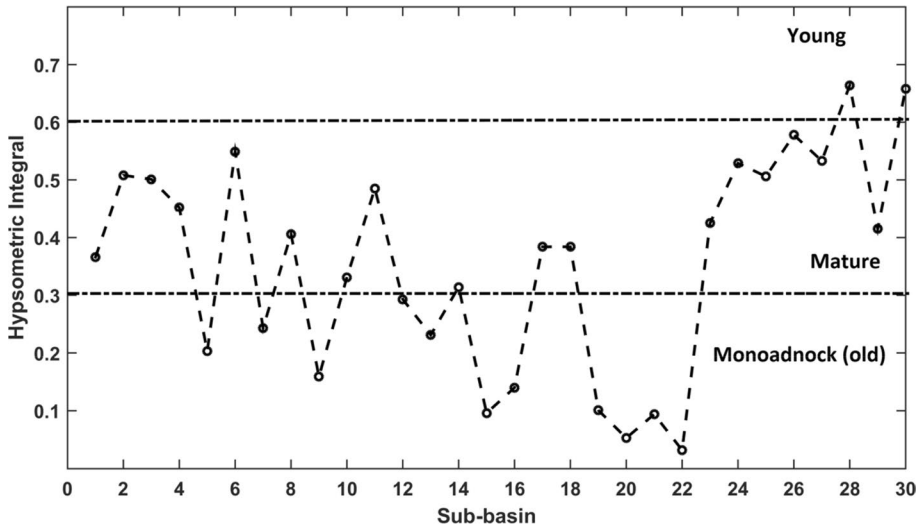


Fig. 11 A schematic diagram showing hypsometric integral (HI) at sub-basin level in the study area

SRTM 30 m and ALOS 30 m DEMs show the 13.98% and 26.38% difference, respectively, from the observed data. In comparison, 90 m resolution DEMs as SRTM and MERIT show the higher differences from observed data and therefore represent the poor results. Hence, it can be concluded that the RULSE results for the SRTM 30 m DEMs followed by the ALOS 30 m are best suited for the Ghaghara river basin. The outcomes from the study are helpful in selection of appropriate DEMs and showed the effects of DEMs variability for soil erosion in basin. It can be concluded that fine resolution DEMs represent good results than the coarser DEMs in basin (Mondal et al. 2017), and hence, the prioritization of basin based on soil erosion will be helpful for recognition of vulnerable areas.

The hypsometric analyses help to know the disequilibria and landscape evolution in the Ghaghara river basin, and there are three types of hypsometric curves according to the geomorphic age of the river basin. Strahler (1952) described the convex upward shape curve for the young stage, while S shape curves for the mature stage have the upper portion concavity while the lower portion convexity. For the old stage (peneplain/monadnock) of the basin, the concave upward shape was suggested by Strahler (1952). Here, in the Ghaghara river basin most of the hypsometric curves of sub-basins are of all three types. Although not all the sub-basins are S-shaped, some are convex upward (sub-basins 28 and 30), and some others are concave upward following the equilibrium condition. The hypsometric integral (HI) values also help to grasp the geomorphic condition of the basin therefore plotted for 30 sub-basins. The HI values validate the same results as the hypsometric curves and the maximum sub-basins of the Ghaghara river basin occupy their position in the mature stage of the erosion cycle and moving toward the monadnock (old stage). Ritter et al. (2002) stated that these mature stages sub-basins would face moderate erosion but might be intense in the high runoff period or in the case of entrenched meandering. Therefore, the HC and HI are useful parameters to understand sub-basin health. The Ghaghara river basin occupies its position in the Himalayan region particularly in the lesser and Shivalik range, and these areas attain the mature stage from the young.

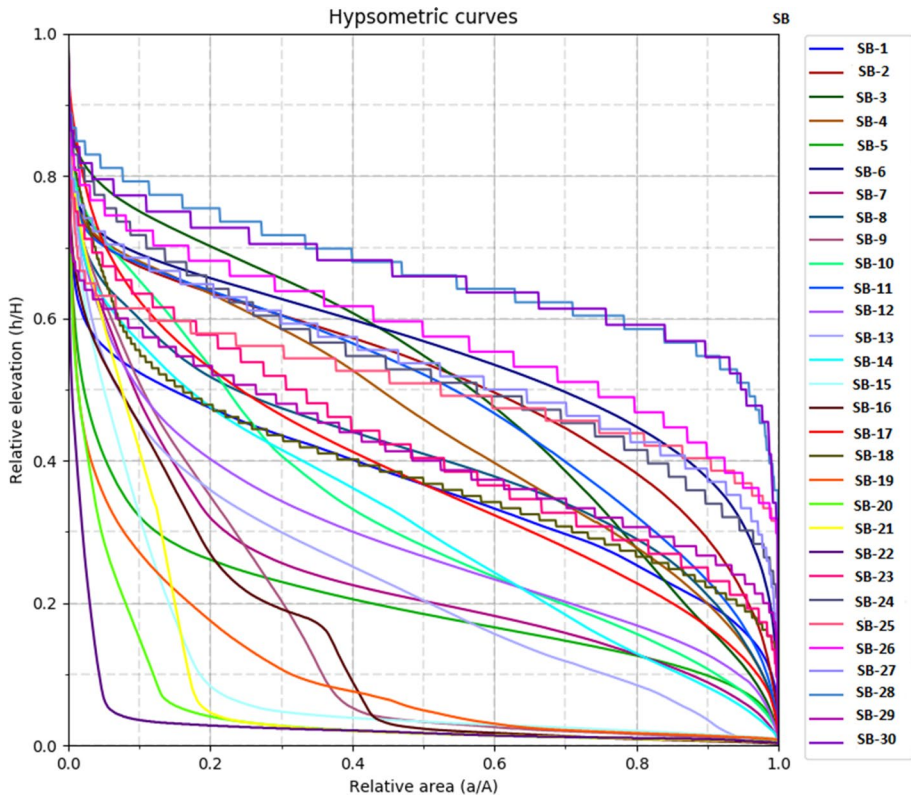


Fig. 12 Sub-basin-wise hypsometric curve in the Ghaghara river basin

Table 5 Percentage-wise soil erosion zone in the Ghaghara river basin

Categories	Area (km <sup>2</sup> )	Area (%)
Very low	4460.0	3.51
Low	51,391.9	40.41
Moderate	59,410.1	46.72
High	11,825.4	9.30
Very high	75.5	0.06
Total	127,162.8	100

### 5 Recommendations and suggestions

The water erosion structure needs to be installed at the soil prone areas, stopping illegal sand mining by implementing the stringent rules and regulations; better understanding about the extreme event and return period of flood is required. The sustainable land use practices need to be focused in the region with no tillage activities, to control the forest clearing, and afforestation activities need to be promoted to intact soil particles. For arrest of lateral erosion, the levee formation and routing of excess water through canals at the time of peak



discharge are recommended. The location-specific process-based models can be applied to allow the use of local parameters governing more erosion in that area. Moreover, the location specific model should use the input of those processes that are actually occurring in study area like landslides and mass wasting which are common processes that are occurring in the Ghaghara river basin. The high resolution of satellite data and DEM is recommended for the estimation of soil erosion to minimize the uncertainty in the results. The downstream siltation records of dams and reservoirs needed for more precise outcomes.

## 6 Conclusion

Estimation of soil erosion will be helpful to control soil loss in the Ghaghara river basin. Therefore, the current study has used RUSLE model for four DEMs to estimate soil loss in the basin. The other parameters, such as morphometric analysis and water holding capacity of soil, have also been calculated. Further, AHP-based MCE methodology has been adopted using three factors (soil loss from RUSLE, compound factor from morphometric analysis, and water holding capacity of soil) to identify soil erosion zone for subsequent conservation measures. The estimated annual soil erosion rates are 21.39, 18.31, 4.35, and 4.64 ton/ha/year for SRTM 30 m, ALOS 30 m, MERIT 90 m, and SRTM 90 m, respectively. The result of erosion rate for the SRTM 30 m DEM is more closed to observed data followed by the ALOS 30 m, while the coarse resolution DEMs depict the poor result. The prioritized map shows the five soil erosion areas which will be helpful in finding the erosion prone zone in the basin. The hypsometric analysis outcomes depict the geomorphic age of basin as old and mature stages form young. The study outcomes will be useful for researchers in appropriate selection of DEMs and to know the consistency in the model outputs due to different resolution DEMs from the observation data.

## Appendix

See Tables 6, 7, 8,9 and 10.

**Table 6** The soil types, their areal distribution in km<sup>2</sup> and percentage, and soil texture in the study area

Soil types	Area (km <sup>2</sup> )	Area (%)	Texture
Bd29-3c-3661	10,384.07	8.08	CLAY_LOAM
Bd34-2bc-3663	22,516.69	17.52	LOAM
Bd35-1-2b-3664	3970.02	3.09	LOAM
Be74-2a-3675	27.56	0.02	LOAM
Be84-2a-3685	41,275.75	32.12	LOAM
Bk39-2a-3694	5207.00	4.05	LOAM
Bk40-2a-3695	43.93	0.03	LOAM
I-Bh-U-c-3717	23,190.87	18.05	LOAM
I-X-2c-3731	214.09	0.17	LOAM
Jc50-2a-3743	315.81	0.25	LOAM
Je75-2a-3759	9361.77	7.29	LOAM
Rd30-2b-3851	7276.55	5.66	CLAY_LOAM
GLACIER-6998	4716.10	3.67	UWB

**Table 7** Land use/land cover classes, areal percentage, and their SWAT code in the study area

Land use classes	Area (km <sup>2</sup> )	Area (%)	SWAT code
Water	74.12	0.058	WATR
Evergreen needle leaf forest	62.22	0.048	FOEN
Evergreen broadleaf forest	15.2	0.012	FOEB
Deciduous needle leaf forest	4.68	0.004	FODN
Deciduous broadleaf forest	7.02	0.005	FODB
Mixed forests	34,083.55	26.52	FRST
Closed shrubland/Open Shrubland	667.05	0.52	SHRB
Woody savannas/savannas	7115.59	5.54	SAVA
Grasslands	22,373.49	17.41	GRASS
Permanent wetland	128.14	0.10	WETL
Croplands	49,269.48	38.34	AGRL
Urban and built-up	381.71	0.29	URBN
Cropland/natural vegetation mosaic	6167.68	4.80	CRWO
Snow and ice	3568.13	2.78	ICES
Barren or sparsely vegetated	4581.58	3.57	BSVG

**Table 8** Basic parameters of morphometry used in the Ghaghara river basin

Sub basin number	I Order stream number	II Order stream number	III Order stream number	IV Order stream number	V Order stream number	Total stream number	I Order stream length (km)	II Order stream length (km)	III Order stream length (km)	IV Order stream length (km)	V Order stream length (km)	Total stream length (km)	Area(A) (km <sup>2</sup> )	Perimeter(P) (km)	Basin Length (L <sub>b</sub> ) (km)
1	17	9	6			32	190.844	135.32	45.062			371.226	4305.86	550.82	152.08
2	9	5	6			20	118.974	68.167	82.028			269.169	2674.69	438.72	116.05
3	20	11	7	3		41	242.68	124.59	112.9	40.75		520.92	6103.04	558.36	185.41
4	19	9	11	4		43	131.12	131.21	139.41	43.16		444.9	4798.28	570.73	161.73
5	17	10	6			33	174.71	101.24	77.76			353.71	3814.01	485.89	141.96
6	14	10	3			27	125.41	97.49	32.75			255.65	3546.04	488.41	136.21
7	12	6	1	7		26	191.06	82.84	19.63	76.71		370.24	3829.62	502.57	142.29
8	14	3	5	7		29	232.42	41.12	76.65	71.02		421.21	4963.91	532.71	164.88
9	18	8	2	9		37	236.43	145.43	64.59	248.78		695.23	5333.12	812.68	171.73
10	25	8	16			49	282.51	123.17	174.11			579.79	6992.31	558.71	200.29
11	31	20	10			61	196.48	214.71	113.74			524.93	6927.41	677.98	199.24
12	10	4	3	8		25	105.71	62.68	37.36	144.84		350.59	2927.69	435.49	122.15
13	21	7	1	15	2	46	239.32	66.39	15.7	228.88	67.73	618.02	5509.75	907.75	174.94
14	10	5	3	3		21	184.57	53.11	40.58	39.11		317.37	3384.49	500.59	132.64
15	17	8	8		2	35	188.35	79.57	76.91		25.75	370.58	3107.01	425.81	126.35
16	23	9	13			45	363.91	192.52	310.64			867.07	7381.67	1142.35	206.56
17	14	10	2			26	125.55	145.75	49.66			320.96	3411.39	385.99	133.24
18	30	12	2	3	17	64	546.61	192.59	99.33	110.13	238.27	1186.93	9240.95	1240.11	234.67
19	25	5	20			50	263.32	64.87	370.92			699.11	5832.59	694.49	180.69
20	22	12	7	2		43	264.52	147.13	144.53	44.62		600.8	4614.23	637.81	158.18
21	18	11	4	5		38	268.96	190.64	43.28	92.58		595.46	4223.79	654.13	150.43
22	13	9	3			25	98.31	149.22	42.85			290.38	2792.15	506.16	118.91
23	6	2	5	1		14	86.14	79.65	194.55	16.61		376.95	2799.74	497.73	119.09
24	11	6	1		5	23	291.54	135.13	7.88		112.58	547.13	4248.29	710.45	150.92
25	7	4	1	5		17	193.74	67.28	7.91	120.59		389.52	2146.05	386.17	102.41

Table 8 (continued)

Sub basin number	I Order stream number	II Order stream number	III Order stream number	IV Order stream number	V Order stream number	Total stream number	I Order stream length	II Order stream length	III Order stream length	IV Order stream length	V Order stream length	Total stream length (km)	Area(A) (km <sup>2</sup> )	Perimeter(P) (km)	Basin Length (L <sub>b</sub> ) (km)
26	6	5				11	168.59	90.08				258.67	2430.32	570.91	109.89
27	9	3		6	8	26	203.91	92.22		166.02	185.81	647.96	4700.53	892.51	159.85
28	9	4		3	7	23	116.56	33.29		31.18	104.17	285.2	1943.26	649.82	96.79
29	15	5	9		2	31	166.89	79.52	101.87		37.41	385.69	3559.33	642.29	136.49
30	3	1			3	7	68.92	17.19			31.45	117.56	958.71	349.76	64.79
Total	465	221	155	81	46	968	6068.06	3204.12	2482.6	1474.98	803.17	14,032.91	128,500.2	3471.55	1046.63

**Table 9** Morphometric parameters in the Ghaghara river basin

Sub-basin number	Linear parameter					Shape parameter				
	$R_b$	$R_L$	$D_d$	$L_o$	$S_f$	$F_f$	$R_e$	$R_c$	$B_s$	$C_c$
1	1.691	0.524	0.086	0.043	0.007	0.186	0.487	0.178	5.372	2.368
2	1.312	0.894	0.101	0.050	0.007	0.199	0.503	0.175	5.035	2.393
3	1.901	0.594	0.085	0.043	0.007	0.178	0.475	0.246	5.633	2.016
4	1.891	0.795	0.093	0.046	0.009	0.183	0.483	0.185	5.451	2.324
5	1.684	0.674	0.093	0.046	0.009	0.189	0.491	0.203	5.284	2.219
6	2.372	0.563	0.072	0.036	0.008	0.191	0.493	0.187	5.232	2.314
7	2.713	1.522	0.097	0.048	0.007	0.189	0.491	0.190	5.287	2.291
8	1.991	0.984	0.085	0.042	0.006	0.183	0.482	0.220	5.476	2.133
9	2.164	1.625	0.130	0.065	0.007	0.181	0.480	0.101	5.530	3.139
10	1.833	0.923	0.083	0.041	0.007	0.174	0.471	0.281	5.738	1.885
11	1.772	0.812	0.076	0.038	0.009	0.175	0.471	0.189	5.730	2.298
12	1.401	1.72	0.120	0.060	0.009	0.196	0.500	0.194	5.097	2.270
13	4.392	3.822	0.112	0.056	0.008	0.180	0.479	0.084	5.555	3.450
14	1.551	0.661	0.094	0.047	0.006	0.192	0.495	0.170	5.199	2.427
15	2.122	0.573	0.119	0.060	0.011	0.195	0.498	0.215	5.138	2.155
16	1.622	1.062	0.117	0.059	0.006	0.173	0.469	0.071	5.780	3.751
17	3.203	0.751	0.094	0.047	0.008	0.192	0.494	0.288	5.204	1.864
18	2.331	1.034	0.128	0.064	0.007	0.168	0.462	0.075	5.959	3.639
19	2.621	2.984	0.120	0.060	0.009	0.179	0.477	0.152	5.598	2.565
20	2.354	0.611	0.130	0.065	0.009	0.184	0.484	0.142	5.422	2.649
21	1.730	1.021	0.141	0.070	0.009	0.187	0.487	0.124	5.358	2.839
22	2.224	0.903	0.104	0.052	0.009	0.197	0.501	0.137	5.064	2.702
23	2.803	1.171	0.135	0.067	0.005	0.197	0.501	0.142	5.066	2.654
24	2.671	4.934	0.129	0.064	0.005	0.187	0.487	0.106	5.362	3.075
25	1.981	5.513	0.182	0.091	0.008	0.205	0.510	0.181	4.886	2.352
26	1.205	0.532	0.106	0.053	0.005	0.201	0.506	0.094	4.970	3.267
27	1.424	1.122	0.138	0.069	0.006	0.184	0.484	0.074	5.436	3.672
28	1.205	1.621	0.147	0.073	0.012	0.207	0.514	0.058	4.821	4.158
29	2.681	0.711	0.108	0.054	0.009	0.191	0.493	0.108	5.234	3.037
30	1.672	1.035	0.123	0.061	0.007	0.228	0.539	0.098	4.379	3.187
Total	1.821	0.610	0.109	0.055	0.008	0.117	0.386	0.134	8.525	2.732

**Table 10** Calculation of compound factor and prioritized ranking of the sub-basins

Linear parameter ranking						Shape parameter ranking					Compound factor	Prioritized rank
Sub-basins no.	R <sub>b</sub>	R <sub>L</sub>	D <sub>d</sub>	L <sub>o</sub>	S <sub>f</sub>	F <sub>f</sub>	R <sub>e</sub>	C <sub>r</sub>	B <sub>s</sub>	C <sub>c</sub>		
1	21	30	25	25	16	13	13	18	18	13	19.2	28
2	28	18	19	19	17	26	26	17	5	14	18.9	27
3	16	26	26	26	18	5	5	28	26	3	17.9	24
4	17	20	23	23	3	9	10	20	21	11	15.7	17
5	22	23	24	24	4	16	16	25	14	6	17.4	22
6	8	28	30	30	12	18	18	21	12	10	18.7	26
7	4	8	20	20	19	17	17	23	15	8	15.1	13
8	14	15	27	27	24	10	9	27	22	4	17.9	25
9	12	6	6	6	20	8	8	8	23	23	12	3
10	18	16	28	28	21	3	3	29	28	2	17.6	23
11	19	19	29	29	5	4	4	22	27	9	16.7	20
12	27	5	11	11	6	23	23	24	8	7	14.5	11
13	1	3	15	15	13	7	7	5	24	26	11.6	2
14	25	24	21	21	25	20	21	16	10	15	19.8	29
15	13	27	13	12	2	22	22	26	9	5	15.1	14
16	24	11	14	14	26	2	2	2	29	29	15.3	16
17	2	21	22	22	14	21	20	30	11	1	16.4	19
18	10	13	9	8	22	1	1	4	30	27	12.5	6
19	7	4	12	13	7	6	6	15	25	16	11.1	1
20	9	25	7	7	8	11	11	13	19	17	12.7	7
21	20	14	3	3	9	14	14	11	16	20	12.4	5
22	11	17	18	18	10	24	24	12	6	19	15.9	18
23	3	9	5	5	28	25	25	14	7	18	13.9	10
24	6	2	8	9	29	15	15	9	17	22	13.2	8
25	15	1	1	1	15	28	28	19	3	12	12.3	4
26	29	29	17	17	30	27	27	6	4	25	21.1	30
27	26	10	4	4	27	12	12	3	20	28	14.6	12
28	30	7	2	2	1	29	29	1	2	30	13.3	9
29	5	22	16	16	11	19	19	10	13	21	15.2	15
30	23	12	10	10	23	30	30	7	1	24	17	21

**Acknowledgements** The authors express their gratitude toward DST-INSPIRE fellowship (No. DST/INSPIRE Fellowship/2016/IF160401), New Delhi, for research encouragement. We are thankful to Central Water Commission, New Delhi, India for providing the sediment data. Author (SKS) has received funding from SERB, New Delhi, India, (Grant no. CRG/2019/003551). We thanks to Dr. Sk Mustak, Dr. Ram L Ray, Prof. Szilard Szabo, and Dr. Rimuka Dzwairo for helping in improving the manuscript.

## References

- Abriha D, Kovacs Z, Ninsawat S, Bertalan L, Balazs B, Szabo S (2018) Identification of roofing materials with discriminant function analysis and random forest classifiers on pan-sharpened worldview-2 imagery—a comparison. *Hung Geogr Bull* 67(4):375–392
- Adhikary PP, Chakraborty D, Kalra N, Sachdev C, Patra A, Kumar S, Tomar R, Chandna P, Raghav D, Agrawal K (2008) Pedotransfer functions for predicting the hydraulic properties of Indian soils. *Soil Res* 46:476–484
- Bali R, Agarwal K, Nawaz Ali SN, Rastogi S, Krishna K (2012) Drainage morphometry of himalayan glacio-fluvial basin, India—hydrologic and neotectonic implications. *Environ Earth Sci* 66:1163–1174
- Barman BK, Bawri GR, Rao KS, Singh SK, Patel D (2021) Drainage network analysis to understand the morphotectonic significance in upper Tuirial watershed, Aizawl, Mizoram. In: *Agricultural Water Management*. Academic Press, pp 349–373
- Bertalan L, Novak TJ, Nemeth Z, Rodrigo-Comino J, Kertesz A, Szabo S (2018) Issues of meander development: land degradation or ecological value? The example of the Sajó River. *Hung Water* 10(11):1–21
- Bertalan L, Rodrigo-Comino J, Surian N, Michalkova MS, Kovacs Z, Szabo S, Szabo G, Hooke J (2019) Detailed assessment of spatial and temporal variations in river channel changes and meander evolution as a preliminary work for effective floodplain management. The example of Sajo River. *Hung J Environ Manage* 248:1–19. <https://doi.org/10.1016/j.jenvman.2019.109277>
- Biesemans J, Van Meirvenne M, Gabriels D (2000) Extending the RUSLE with the Monte Carlo error propagation technique to predict long term average off-site sediment accumulation. *J Soil Water Conserv* 55:35–42
- Borrelli P, Robinson DA, Fleischer LR, Lugato E, Ballabio C, Alewell C, Meusburger K, Modugno S, Schutt B, Ferro V, Bagarello V, Oost KV, Montanarella L, Panagos P (2017) An assessment of the global impact of 21st century land use change on soil erosion. *Nat Commun* 8:1–13. <https://doi.org/10.1038/s41467-017-02142-7>
- Brady CN, Weil RR (2008) *The nature and properties of soils*, 14th edn. Prentice Hall, USA
- Choubey VM, Ramola RC (1997) Correlation between geology and radon levels in groundwater, soil and indoor air in Bhilangana valley, Garhwal Himalaya, India. *Environ Geol* 32:258–262
- Choudhari PP, Nigam GK, Singh SK, Thakur S (2018) Morphometric based prioritization of sub-basin for groundwater potential of Mula river basin, Maharashtra, India. *Geol, Ecol, Landsc* 2(4):256–267. <https://doi.org/10.1080/24749508.2018.1452482>
- Ciesiolka CA, Coughlan KJ, Rose CW, Escalante MC, Hashim GM, Paningbatan EP, Sombatpanit S (1995) Methodology for a multicountry study of soil erosion management. *Soil Technol* 8:179–192
- Dash B, Nagaraju MSS, Sahu N, Nasre RA, Mohekar DS, Srivastava R, Singh SK (2019) Morphometric analysis for planning soil and water conservation measures using geospatial technique. *Int J Curr Microbiol App Sci* 8(1):2719–2728
- De RA, Jetten V, Wesseling C, Ritsema C (1998) LISEM: A physically-based hydrologic and soil erosion catchment model. In *Modeling Soil Erosion by Water*. In: Boardman J, Favis Mortlock D (Eds) (pp. 429–440) Springer, Berlin, Germany
- Degetto M, Gregoretti C, Bernard M (2015) Comparative analysis of the differences between using LiDAR and contour-based DEMs for hydrological modeling of runoff generating debris flows in the Dolomites. *Front Earth Sci* 3
- Desmet PJJ, Govers G (1996) A GIS procedure for automatically calculating the USLE LS factor on topographically complex landscape units. *J Soil Water Conserv* 51(5):427–433
- Dowling TI, Richardson DP, OSullivan A, Sumnerell GK, Walker J (1998) Application of the hypsometric integral and other terrain based metrics as indicators of the Catchment health: A preliminary analysis. CSIRO Land and Water, Technical Report 20/98. Canberra
- FAO/UNESCO (1977) *Soil Map of the World, Volume VI. Africa*. Rome: FAO; Paris: UNESCO
- Gajbhiye S, Mishra SK, Pandey A (2014) Prioritizing erosion-prone area through morphometric analysis: an RS and GIS perspective. *Appl Water Sci* 4:51–61. <https://doi.org/10.1007/s13201-013-0129-7>
- Gitas IZ, Douros K, Minakou C, Silleos GN, Karydas CG (2009) Multi-temporal soil erosion risk assessment in N. Chalkidiki using a modified USLE raster model. *EARSeL Proceedings* 8
- Goepel K (2018) Implementation of online software tool for the analytic hierarchy process (AHP-OS). *Int J Anal Hierarchy Process* 10(3):1–5. <https://doi.org/10.13033/ijahp.v10i3.590>
- Gravelius H (1914) *Grundrifi der gesamten Gewisserkunde. Band I: Flufikunde (Compendium of Hydrology, Vol. I. Rivers, in German)*. Goschen, Berlin, Germany
- Gupta M, Srivastava PK (2010) Integrating GIS and remote sensing for identification of groundwater potential zones in the hilly terrain of Pavagarh, Gujarat, India. *Water Int* 35:233–245

- Horton RE (1932) Drainage-basin characteristics trans am geophys union. *Trans, Am Geophys Union* 13:350–361
- Horton RE (1945) Erosion development of streams and their drainage basins; hydrophysical approach to quantitative morphology. *Geol Soc Am Bull* 56:275–370
- Jain SK, Kumar S, Varghese J (2001) Estimation of soil erosion for a Himalayan sub-basin using GIS technique. *Water Resour Manag* 15:41–54
- Knisel WG (1980) CREAMS: a field scale model for chemicals, runoff, and erosion from agricultural management systems (No. 26). Department of Agriculture, Science and Education Administration
- Koirala P, Thakuri S, Joshi S, Chauhan R (2019) Estimation of soil erosion in Nepal using a RUSLE modeling and Geospatial Tool. *Geosci J* 9:1–19. <https://doi.org/10.3390/geosciences9040147>
- Kosmas C, Danalatos N, Cammeraat HN, Chabart M, Diamantopoulos J, Faand R, Gutierrez L, Jacob A, Marques H, Fernandez JM, Mizara A, Moustakas N, Niclau JM, Oliveros C, Pinna G, Puddu R, Puigdefabrgas J, Roxo M, Simao A, Stamou G (1997) The effect of land use on runoff and soil erosion rates under Mediterranean conditions. *CATENA* 29(1):45–59. [https://doi.org/10.1016/S0341-8162\(96\)00062-8](https://doi.org/10.1016/S0341-8162(96)00062-8)
- Kumar N, Singh SK, Srivastava PK, Narsimlu B (2017) SWAT model calibration and uncertainty analysis for stream flow prediction of the Tons river basin, India, using sequential uncertainty fitting (SUFI-2) algorithm. *Model Earth Syst Environ* 3(30):1–13. <https://doi.org/10.1007/s40808-017-0306-z.s>
- Kumar M, Denis DM, Singh SK, Szabo S, Suryavanshi S (2018) Landscape metrics for assessment of land cover change and fragmentation of a heterogeneous sub-basin. *Remote Sens Appl: Soc Environ* 10:224–233
- Kumar D, Singh DS, Prajapati SK, Khan I, Gautam PK, Vishwakarma B (2018) Morphometric parameters and neotectonics of Kalyani river basin, Ganga plain: a remote sensing and GIS approach. *J Geol Soc India* 91(6):679–686
- Kumar N, Singh SK, Singh VG, Dzwairo B (2018a) Investigation of impacts of land use/land cover change on water availability of Tons River Basin, Madhya Pradesh, India. *Model Earth Syst Environ* 4:295–310
- Kumar N, Singh SK, Pandey HK (2018b) Drainage morphometric analysis using open access earth observation datasets in a drought-affected part of Bundelkhand, India. *Appl Geomat* 10:173–189. <https://doi.org/10.1007/s12518-018-0218-2>
- Laen JM, Lane LJ, Foster GR (1991) WEPP: a new generation of erosion prediction technology. *J Soil Water Conserv* 46(1):34–38
- Li Z, Fang H (2016) Impacts of climate change on water erosion: a review. *Earth Sci Rev* 163:94–117
- Liu Y, Guo Y, Li Y, Li Y (2015) GIS-based effect assessment of soil erosion before and after gully land consolidation: a case study of Wangjiagou project region. *Loess Plateau Chin Geogr Sci* 25(2):137–146
- Lu D, Li G, Valladares GS, Batistella M (2004) Mapping soil erosion risk in Rondônia, Brazilian Amazonia: using RUSLE, remote sensing and GIS. *Land Degrad Dev* 15(5):499–512
- Mahapatra GB (2005) Text book of physical geology. CBS Publishers & Distributors, Bengaluru
- Maliqi E, Singh SK (2019) Quantitative estimation of soil erosion using open-access earth observation datasets and erosion potential model. *Water Conser Sci Eng* 4(4):187–200
- Maurya S, Srivastava PK, Gupta M, Islam T, Han D (2016) Integrating soil hydraulic parameter and microwave precipitation with morphometric analysis for sub-basin prioritization. *Water Resour Manage* 30:5385–5405. <https://doi.org/10.1007/s11269-016-1494-4>
- Moglen GE, Eltahir EA, Bras RL (1998) On the sensitivity of drainage density to climate change. *Water Res* 34:855–862
- Mondal A, Khare D, Kundu S (2017) Uncertainty analysis of soil erosion modelling using different resolution of open-source DEMs. *Geocarto Int* 32(3):334–349
- Morgan RPC, Morgan DDV, Finney HJ (1984) A predictive model for the assessment of soil erosion risk. *J Agric Eng Res* 30:245–253
- Morgan RPC, Quenton JN, Rickson RJ (1992) EUROSEM: documentation manual. Silsoe, UK
- Murmu P, Kumar M, Lal D, Sonker I, Singh SK (2019) Delineation of groundwater potential zones using geospatial techniques and analytical hierarchy process in Dumka district, Jharkhand. *India Groundw Sustain Dev* 9:100239. <https://doi.org/10.1016/j.gsd.2019.100239>
- Nag SK (1998) Morphometric analysis using remote sensing techniques in the Chaka sub-basin, Purulia district, West Bengal. *J Indian Soc Remote Sens* 26(1–2):69–76
- Nag SK, Chakraborty S (2003) Influence of rock type and structure development of drainage network in hard rock terrain. *J Indian Soc Remote Sens* 31(1):25–35



- Nyakatawa EZ, Reddy KC, Lemunyon JL (2001) Predicting soil erosion in conservation tillage cotton production systems using the revised universal soil loss equation (RUSLE). *Soil Tillage Res* 57(4):213–224
- Panagos P, Borrelli P, Meusburger K, Alewell K, Lugato E, Montanarella L (2015a) Estimating the soil erosion cover-management factor at the European scale. *Land Use Policy* 48:38–50. <https://doi.org/10.1016/j.landusepol.2015.05.021>
- Panagos P, Borrelli P, Poesen J, Ballabio C, Lugato E, Meusburger K, Montanarella L, Alewell C (2015b) The new assessment of soil loss by water erosion in Europe environmental science & Policy. *Environ Sci Policy* 54:438–447. <https://doi.org/10.1016/j.envsci.2015.08.012>
- Panagos P, Borrelli P, Poesen J (2019) Soil loss due to crop harvesting in the European Union: a first estimation of an underrated geomorphic process. *Sci Total Environ* 664:487–498
- Parveen R, Kumar U (2012) Integrated approach of universal soil loss equation (USLE) and geographical information system (GIS) for soil loss risk assessment in upper south Koel Basin, Jharkhand. *J Geogr Inf Syst* 4:588–596
- Perovic V, Zivotic L, Kadovic R, Dordevic A, Jaramaz D, Mrvic V (2013) Spatial modelling of soil erosion potential in a mountainous sub-basin of South-eastern Serbia. *Environ Earth Sci* 68:115–128. <https://doi.org/10.1007/s12665-012-1720-1>
- Phinzi K, Abriha D, Bertalan L, Holb I, Szabo S (2020) Machine learning for gully feature extraction based on a pan-sharpened multispectral image: multiclass vs. Bin Approach. *Int J Geo-Inf* 9(4):252. <https://doi.org/10.3390/ijgi9040252>
- Pike RJ, Wilson SE (1971) Elevation-relief ratio, hypsometric-integral and geomorphic area-altitude analysis. *Geological Soc Am Bull* 82:1079–1084
- Pradhan RK, Srivastava PK, Maurya S, Singh SK, Patel DP (2018) Integrated framework for soil and water conservation in Kosi River Basin. *Geocarto Int* 35(4):391–410. <https://doi.org/10.1080/10106049.2018.1520921>
- Quantum GIS (2019) Development Team (2014) QGIS Geographic Information System. Open Source Geospatial Foundation Project. Online at:
- Rao NS (2016) Hydrogeology: problems with solutions. PHI Learning Pvt Ltd, Delhi
- Ratnam KN, Srivastava Y, Rao VV, Amminedu E, Murthy K (2005) Check dam positioning by prioritization of micro-sub-basins using SYI model and morphometric analysis—remote sensing and GIS perspective. *J Indian Soc Remote Sens* 33(1):1–38
- Rawat KS, Singh SK, Singh Mlc, Garg BL (2019) Comparative evaluation of vertical accuracy of elevated points with ground control points from ASTERDEM and SRTMDEM with respect to CARTOSAT-1DEM. *Remote Sens Appl: Soc Environ* 13(289):297
- Rawat KS, Singh SK, Szilard S (2020) Comparative evaluation of models to estimate direct runoff volume from an agricultural watershed. *Geol, Ecol, Lands*. <https://doi.org/10.1080/24749508.2020.1833629>
- Raymo ME, Ruddiman WF (1992) Tectonic forcing of Late Cenozoic climate. *Nature* 359:117–122
- Reddy GPO, Maji AK, Gajbhiye KS (2004) Drainage morphometry and its influence on landform characteristics in a basaltic terrain, Central India—A remote sensing and GIS approach. *Int J Appl Earth Obs* 6(1):1–16. <https://doi.org/10.1016/j.jag.2004.06.003>
- Renard KG, Foster GR, Weesies GA, Porter JP (1991) RUSLE: Revised universal soil loss equation. *J Soil Water Conserv* 46(1):30–33
- Renard KG, Foster GR, Weesies GA, McCool DK, Yoder DC (1996) Predicting soil erosion by water: a guide to conservation planning with the Revised Universal Soil Loss Equation (RUSLE). *Agric Handb* 703:25–28
- Ritter DF, Kochel RC, Miller JR (2002) Process geomorphology. McGraw Hill, Boston
- Saaty T (1980) The analytic hierarchy process. McGraw-Hill, New York
- Saaty TL, Vargas LG (1980) Hierarchical analysis of behavior in competition: prediction in chess. *Syst Res Behav Sci* 25:180–191
- Schaap MG, Leij FJ, Van Genuchten MT (2001) ROSETTA: a computer program for estimating soil hydraulic parameters with hierarchical pedotransfer functions. *J Hydrol* 251(3–4):163–176
- Schlosser AD, Szabo G, Bertalan L, Varga Z, Enyedi P, Szabo S (2020) Building extraction using orthophotos and dense point cloud derived from visual band aerial imagery based on machine learning and segmentation. *Remote Sens* 12(15):1–28. <https://doi.org/10.3390/rs12152397>
- Schumm SA (1956) Evolution of drainage systems and slopes in badlands at Perth Amboy, New Jersey. *Geol Soc Am Bull* 67:597–646
- Schuol J, Abbaspour KC, Srinivasan R, Yang H (2008) Modelling blue and green water availability in Africa at monthly intervals and subbasin level. *Water Res Res* 44:W07406. <https://doi.org/10.1029/2007WR006609>

- Sethupathi AS, Narasimhan CL, Vasanthamohan V, Mohan SP (2011) Prioritization of mini sub-basins based on morphometric analysis using remote sensing and GIS techniques in a draught prone Bargur—Mathur sub-basins, Ponnaiyar River basin, India. *Int J Geomatics Geosci* 2:403–414
- Sharpley AN, Williams JR (1990) EPIC-Erosion/Productivity impact calculator. I: Model documentation. II: User manual. Technical Bulletin-United States Department of Agriculture, (1768)
- Singh DS, Awasthi A (2011) Implication of drainage basin parameters of Chhoti Gandak River, Ganga Plain, India *J Geol Soc India* 78(4):370–378
- Singh P, Thakur JK, Singh UC (2013) Morphometric analysis of Morar River Basin, Madhya Pradesh, India, using remote sensing and GIS techniques. *Environ Earth Sci* 68(7):1967–1977
- Singh V, Singh SK (2018) Hypsometric Analysis Using Microwave Satellite Data and GIS of Nainagorma River Basin (Rewa district, Madhya Pradesh, India). *Water Conserv Sci Eng* 3(4):221–234
- Srivastava PK, Han D, Gupta M, Mukherjee S (2012) Integrated framework for monitoring groundwater pollution using a geographical information system and multivariate analysis. *Hydrol Sci J* 57:1453–1472
- Strahler AN (1952) Hypsometric (area-altitude) analysis of erosional topography. *Geologic Soc Am Bull* 63:1117–1141
- Strahler AN (1964) Quantitative geomorphology of drainage basins and channel networks. In: Chow VT (ed) *Handbook of applied hydrology*. McGraw Hill, New York, pp 39–76
- Szabó G, Singh SK, Szabó S (2015) Slope angle and aspect as influencing factors on the accuracy of the SRTM and the ASTER GDEM databases. *Phys Chem Earth* 83–84:137–145
- Terranova O, Antronico L, Coscarelli R, Iaquina P (2009) Soil erosion risk scenarios in the Mediterranean environment using RUSLE and GIS: an application model for Calabria (southern Italy). *Geomorphology* 112:228–245
- Thakur JK, Singh SK, Ekanthalu VS (2016) Integrating remote sensing, geographic information systems and global positioning system techniques with hydrological modeling. *Appl Water Sci* 7:1595–1608. <https://doi.org/10.1007/s13201-016-0384-5>
- Thomas J, Joseph S, Thirivikramji KP (2018) Estimation of soil erosion in a rain shadow river basin in the southern Western Ghats, India using RUSLE and transport limited sediment delivery function. *Int Soil Water Conserv Res* 6(2):111–122
- Uddin K, Murthy MSR, Wahid SM, Matin MA (2016) Estimation of soil erosion dynamics in the Koshi Basin using GIS and remote sensing to assess priority areas for conservation. *PLoS ONE* 11(3):e0150494. <https://doi.org/10.1371/journal.pone.0150494>
- Van Genuchten MT (1980) A closed-form equation for predicting the hydraulic conductivity of unsaturated soils. *Soil Sci Soc Amer J* 44:892–898
- Vittala SS, Govindiah S, Honne GH (2004) Morphometric analysis of sub-sub-basins in the pawagada area of Tumkur district, South India, using remote sensing and GIS techniques. *J Indian Soc Remote Sens* 32(4):351–362
- Waikar ML, Nilawar AP (2014) Morphometric analysis of a drainage basin using geographical information system: a case study. *Int J Multidiscip Res dev* 2:178–184
- Wijesundara NC, Abeysingha NS, Dissanayake DMSLB (2018) GIS-based soil loss estimation using RUSLE model: a case of Kirindi Oya river basin. *Sri Lanka Model Earth Syst Environ* 4(1):251–262
- Williams JR (1975) Sediment-yield prediction with universal equation using runoff energy factor. Present and prospective technology for predicting sediment yields and sources, 40:244–52
- Wischmeier WH, Smith DD (1978) Predicting rainfall erosion losses: a guide to conservation planning (No. 537). Department of Agriculture, Science and Education Administration. Hyattsville, MD, USA
- Yadav SK, Singh SK, Gupta M, Srivastava PK (2014) Morphometric analysis of upper tons basin from Northern Foreland of Peninsular India using CARTOSAT satellite and GIS. *Geocarto Int* 29(8):895–914. <https://doi.org/10.1080/10106049.2013.868043>
- Yadav SK, Dubey A, Singh SK, Yadav D (2020) Spatial regionalisation of morphometric characteristics of mini watershed of Northern Foreland of Peninsular India. *Arab J Geosci* 13(12):435. <https://doi.org/10.1007/s12517-020-05365-z>
- Young RA, Onstad C, Bosch D, Anderson W (1989) AGNPS: a nonpoint-source pollution model for evaluating agricultural sub-basins. *J Soil Water Conserv* 44(2):168–173
- Yu B, Rosewell CJ (1996) Technical Notes: a Robust Estimator of the R-factor for the Universal Soil Loss Equation. *Trans ASAE* 39(2):559–561